Response to Reviews – Esurf Manuscript

Effect of rock uplift and Milankovitch timescale variations in precipitation and vegetation cover on catchment erosion rates

By: Sharma et al.

Responses in blue, original comment in black

Response to Associate Editor: Greg Hancock

Dear Prof. Hancock,

We would like to thank you for agreeing to be the associate editor of our manuscript. We also thank our referees, Erkan Istanbulluoglu and Omer Yetemen for their valuable comments and requests for clarification. We hope this will improve the quality of our manuscript and make it more useful to the prospective readers.

Following the constructive criticism and suggestions by the referees, we present here our revised manuscript. We hope it helps with meeting the referee's expectations and fits the high standard of Esurf.

In response to RC1 regarding the lag behaviors in mean catchment sediment entrainment and bedrock erosion rates visible in Fig. 5-9, we revisited the simulations and tested the model to detect the role of state variables leading to these lags. On reading the further comments by Erkan Istanbulluoglu, we emphasized the weathering processes. We observed that if we switch off the weathering function in our coupled simulations, we don't observe evident phase lags in bedrock erosion. In regards to this observation, we added a paragraph to explain the same in Discussion section 4.2, accompanied with a figure A1 (in appendix). We shortened the sentences in our hypotheses and moved them from section 5 "Summary and Conclusions" to section 1 "Introduction" to make it clearer in the introduction itself. Labels (e.g., 10 PV replaced by 10% V) and figure captions are corrected referring to corresponding plots in Fig. 5-11. The distribution of sinusoidal oscillations of mean annual precipitation (MAP) for both wet and dry catchments is explained in the last paragraph of section 2.1 "Model setup and scenarios considered". The phase lag in sediment entrainment and bedrock erosion but no lag in catchment scale erosion is explained briefly in Section 3.1. "Scenario 1".

In response to RC2 we have made the requested changes to our manuscript, which were mostly clarifications, but very important to improve manuscript clarity.

We have provided the details of manuscript revision in the point-by-point response to the referees' comments. We deeply appreciate your and all referees' efforts to help us improve our manuscript.

The submission file consists of our cover letter, followed by point-by-point response to referees' comments, and the revised manuscript (with tracked-changes) specifying all the modifications made in accordance with the referees' comments.

Please contact us if further clarifications are required.

Sincerely,

Hemanti Sharma and Todd Ehlers (corresponding author) on behalf of all co-authors.

Response to RC1

Responses in blue

1. Very good paper. It contributes to our conceptual understanding of climate-veg-weathering-erosion interactions. The authors pose two hypotheses and do extensive model runs to test them. The only comment I have is that the authors explain the model results based on interpretations of what might be happening in the model. For example, they show the lag behaviors in erosion rates (especially in Fig 8,9 – 100 kyr), discuss what might be happening in the model that lead to the lag in erosion but they don't actually prove that by looking at the model state variables themselves that lead to lags. Changes in the landscape relief/mass and slopes are not discussed. Phase diagrams by plotting model evolving model states against each other can be done to further explore the model behavior and causalities. I just put this out there as perhaps for future work for the authors, as this paper is already thick.

   The referee raised a very interesting point to emphasize on the model state variables leading to lag behaviors in sediment entrainment and bedrock erosion rates (e.g., Fig. 5-9), but no lags in overall catchment erosion rates. To address this issue, we performed a new set of simulations without the weathering/regolith production function activated, to determine the sensitivity of our model to the weathering rate (regolith production rate). We observed that it impacts the erosion rates extensively and phase lags in sediment entrainment and bedrock erosion are insignificant without weathering function being active. Hence we deduce that these "lag behaviors" are caused by "weathering function", with maximum regolith production rates, such that densely vegetated catchment would produce more sediment. We added this explanation as a separate paragraph in Discussion section 4.2 (lines 454 - 463) and supporting Figure A1, in Appendix.

   We do not discuss the changes in landscape mass/relief in this paper, as the main objectives of this study were to report the sensitivity of the catchment scale erosion and sedimentation to variable vegetation cover and climate over Milankovitch timescales. And if the transients caused by above are dampened or enhanced at higher rock uplift rates. Also, length of the paper was already overwhelming and the above mentioned phenomenon is already discussed in detail in the similar paper by Schmid et al. (2018). However, adding phase diagrams by plotting the model states against each other would add more insight into model behaviour and casualties. This suggestion is very helpful and will be applied in our future work as suggested by the reviewer.

2. The reference below has some similar work for the authors to include in their discussion, if they see relevant.

   Yetemen O., Saco P., and E. Istanbulluoglu (2019). Ecohydrology controls the geomorphic response to climate change, Geophysical Research Letters, 46.

   We have added the above citation in Section 4.6 (line 541).

3. The authors should check the figure captions to make sure they refer the plots correctly. I had some difficulty relating caption alphabetic references to those on the figures.

Thank you for pointing out this error. It has been corrected in the revised manuscript for Fig 5-11.

4. I suggest you give the hypotheses in shorter sentences and make them clear in the Intro. The summary section had them a lot more direct, perhaps you can move those to intro and shorten a bit.

The hypotheses have been shortened and moved to the introduction (lines 90-108) from the summary section. Hypotheses in the summary section have been re-written in shorter sentences (lines 616 - 620). This helps the reader to understand clearly the objectives of this study by looking at the introduction.

5. In the wetter climate simulations MAP does not follow a perfect sinusoidal function. Why?

We follow the approach of Schmid et al., (2018) in designing the climate and vegetation cover oscillations for coupled simulations. In coupled simulations (coupled vegetation and precipitation oscillations – Scenario 3-5), MAP follows an asymmetrical sinusoidal function for both wet and dry catchments. This is done to isolate the impact of changing precipitation and vegetation cover on erosion rates and sedimentation. This asymmetry is clearly visible in wetter climate simulations because of higher amplitude of change in MAP (i.e., 260 mm – 720 mm) needed to cause an associated vegetation change. In the words, the non-linear relationship between precipitation and vegetation cover observed in Chile (Fig. 2c) is the source of the asymmetry noted by the reviewer. This explanation has been added to the section "2.1. Model setup and scenarios considered" in lines 205 – 210.

6. Fig 5. 10PV. Why not just use 10%V.

10PV and 70PV have been replaced with 10% V and 70% V respectively in Fig. 5, 6, 7.

7. Fig 5. -2ky and +3kyr phase lag for entrainment and bedrock erosion but no lag in the catchment-scale erosion. Did the mean bedrock erosion include weathering? I guess it did not.

Bedrock erosion here includes weathering too (i.e., bedrock converted to sediment using an exponential weathering component in Landlab), which is calibrated to the Chilean Coastal Cordillera observations of Schaller et al., (2018). As we use the total change in bedrock elevation to calculate bedrock erosion rate, the loss in bedrock due to weathering is also accounted for. This explanation has now been added to the section 3.1 (lines 238 - 241).

8. Fig 6. Why is there 5 times higher erosion rate for bare soil. Are these results after spin up using 21kyr periodicity. Because I suspect the low-veg catchment should maintain a lower relief and slopes. The higher veg catchment should develop steeper slopes and when thresholds are exceeded the higher veg catchment could produce more sediment at the outlet. If Fig 6e averaged mean erosion rates that correspond to the same time stamps within each cycle, the area under the curve should have giving you about the same amount of sediment

mass, unless there are details in the weathering function such that vegetated landscape would produce more sediment.

Fig. 6. These results are obtained after the spin up for ~10 cycles of 23 kyr on a steady state topography (with spin up of 15 Myr). Although the relief and slopes were relatively lower for sparsely vegetated catchment (10% V), we got high erosion rates as the precipitation was kept constant at 30 mm yr^{-1}, while the vegetation cover was reduced to 0% (bare soil). This can be attributed to (bedrock/sediment) stream power thresholds, which are model input parameters. The low erosion thresholds might lead to high erosion rates for bare soil. Also, in our model, we do not account for ground percolation, so all the water entered into the system in the form of precipitation is contributing to erosion if thresholds are exceeded. This explanation has been added to Section 3.2 (lines 284 - 286).

In weathering function, the input parameter (maximum soil production rate) is different for both catchments, such that densely vegetated landscape would produce more sediment (W_o) in Table 1 (i.e., 9.7×10^{-6} m yr^{-1} for 10% V and 1.3×10 m yr^{-1} for 70% V). These values of sediment production are taken from the observations of Schaller et al., (2018)

9. Interesting that the dry-phase is all depositional in fig 6, while there is net bedrock erosion during the dry phase… are the bedrock erosion rates happen partially in places where there were no deposition?

Bedrock erosion happens partially in areas with no or low deposition, as documented by Shobe et al., (2017) in the documentation of SPACE component of Landlab. In our model, exposed bedrock is subjected to erosion and weathering (major contributor of bedrock loss in this case). This has been added in lines 278 – 280.

10. Can you please clarify these higher rates in the bare and that if these results are obtained after spin up for 21 kyr.

Please refer to the response to comment #8

11. Fig 8, 9 are very interesting. The double-peak in catchment mean erosion is very interesting, especially with 100kyr cycle which was more clear to detect visually.

The double-peak in catchment mean erosion rates (in sparse vegetation 10% V) in Fig. 8 and 10 are first observed in Fig. 7e (for 10% V), and explained in section 3.2. "Influence of coupled oscillations of precipitation and vegetation cover, on erosion and sedimentation (Scenario 3)" and section 4.2. This is because we use coupled oscillations in precipitation and vegetation cover in the simulations in scenarios 4 for different periodicities (corresponding to Fig. 8), as scenario 5 for different rock uplift rates (corresponding to Fig. 10). We do not observe double peaks in Fig 9, for densely vegetated catchment (70% V).

12. I see that in the discussion section you explain the role of bedrock erosion on higher erosion modeled erosion rate in the sparsely vegetated scenario.
Lines 417-419 – good explanation and a conceptual model. I felt the same while I was looking at the plots.
We are glad that you like the explanation and conceptual model.

13. To add to the limitations – you don't seem to have vegetation disturbance by flow and entrainment. That had a large impact on the simulations of Collins et al 2004 and Istanbulluoglu and Bras 2005. Probably with some veg loss in channels you would have gotten a hybrid result between 10% and 70% veg cases (including their oscillations).

Limitations: We have forced the climate and vegetation oscillations in our model in the style of Schmid et al., (2018). So, here vegetation cover is an input parameter, which is independent of flow an entrainment in the model. Thanks for highlighting this point to add to our model limitations, this makes a caveat in our model worth mentioning. This limitation has been added to Section 4.7 of the revised manuscript (lines 601 - 604).

Response to RC2

Responses in blue

1. This paper investigates how Milankovitch timescale variations in precipitation affect catchment erosion rates via modelling approach. This is a very interesting and very good paper. It will be very good contribution to geomorphology. I have a very minor comments to the authors which are mostly clarification.

We thank the reviewer for the constructive review and pointing out minor but significant errors in our manuscript.

2. L33-35. Hedging required! Please reframe this statement "For example, recent work highlights that higher vegetation and lower precipitation both decrease erosion" with cites because some of them are only focused on bare soil, no vegetation, e.g., Bonnet and Crave (2003).

The sentence has been reframed to "For example, recent work highlights that denser vegetation or lower precipitation both decrease erosion" (lines 34-36). In the above sentence, we meant that both denser vegetation cover and lower precipitation rates (together or independently) result in decreasing erosion rates. So, we referred to the studies which include either climate or vegetation influence on the catchment erosion rates.

3. L63. Hedging required! "As precipitation increases, vegetation cover increases rapidly, and other factors become limiting (Breckle, 2002)." Not necessarily, water limitation can still be the limiting factor!

Thanks for pointing this out. This clarification is added to the revised manuscript (lines 54 - 55) (L63 now changed to L54-55).

4. L67. I recommend relatively recent work (Knapp et al., 2017) about the MAP and ANPP relationship. Also, the same reference can be used in L136-138.

Knapp et al., 2017. Reconciling inconsistencies in precipitation–productivity relationships: implications for climate change. New Phytologist (2017) 214: 41–47

Thanks for recommending Knapp et al., (2017) for the MAP and ANPP relationship. It is a very interesting addition to add as a reference in the explanation of the same in line 59 (L67 now changed to L59) and lines L136-138.

5. L192. Table 1. Porosity value is 0.2. If it defines soil porosity, it is a bit lower than the reported values in the hydrology literature. Is there any reason for low value?

The porosity used in this study is lower than usual range for soil (0.3 – 0.4), as sediment produced as a result of weathering in the study areas is a mixture of fine and coarse grained regolith (Schaller et al., 2020). Hence, we assume lower porosity for sediment in the model. This explanation has been added to Section 2.1. of the revised manuscript (lines 193 - 195).

6. L393-395. I recommend to check Fig 2.g in Yetemen et al. (2015) (support your finding in modelling approach) to show how erosion (shear stress) change as a function of vegetation cover.

Yetemen, O., E. Istanbulluoglu and A.R. Duvall (2015). Solar radiation as a global driver of hillslope asymmetry: Insights from an ecogeomorphic landscape evolution model. Water Resources Research, 51, 9843-9861.

For experimental approach:

Rogers & Schumm (1991). The effect of sparse vegetative cover on erosion and sediment yield. Journal of Hydrology, 123:1-2, 19-24.

Thanks for recommending above mentioned references. Yetemen et al., (2015) been added to the Discussion Section 4.1 (lines 421 - 423) (L393-395 now changed to L413-415) in support of our findings in modeling approach. However, Rogers and Schumm (1991) does not clearly support our findings of higher sensitivity of sparsely vegetated catchments to change from bare soil to 20% vegetation cover. That study suggests no significant change in erosion rates with respect to vegetation cover if vegetation cover < 15%. In this regard, we cannot use Rogers and Schumm (1991) to validate our findings.

7. L556-558. Seasonality in precipitation was introduced in landscape evolution models such as Istanbulluoglu and Bras (2006) Yetemen et al. (2015).

Thanks for pointing this out, these studies are basis of the above statement. "Seasonal variations in precipitation" have been cited with the above mentioned references in the reframed sentence (lines 606 - 609). We intended to talk about the impact of coupled variations in climate (mainly precipitation) and satellite derived vegetation cover (with PFT distribution) on seasonal catchment erosion rates.

MINOR POINTS

8. L33. Word choice. I recommend replacing "denser" for "higher" vegetation.

Corrected in the revised manuscript (line 34)

9. L197. Word choice. I recommend replacing "esteemed from" for "influenced by".

    Corrected in the revised manuscript (line 200)

10. L220. Plural subject. Negative values….correspond….

    Corrected in the revised manuscript (line 229)

11. L296. Insert comma before 'and'. Also L413.

    Corrected in the revised manuscript (lines 316 and 443)

12. L435. Please check. Possible typo? …vegetation driven changes IN erosion will..

    Corrected in the revised manuscript (line 478)

13. L455. Insert comma after. "sections".

    Corrected in the revised manuscript (line 498)

14. L485. Typo! Maybe re-write! "un".

    Corrected in the revised manuscript (line 528)

15. L532. Istanbulluoglu AND BRAS, 2005. Also correct citation L742.

    Corrected in the revised manuscript (line 578 and 796)

16. L532. Is Guzman (2019) a modelling study?

    Thanks for pointing that out. Guzman (2019) is a review article and not a modeling study. The citation has been removed from main text (line 578) and references (line 774-775).

17. L657. Typo. Delete "Gregory".

    Corrected in the revised manuscript (line 706)

Effect of rock uplift and Milankovitch timescale variations in precipitation and vegetation cover on catchment erosion rates

Hemanti Sharma[1], Todd A Ehlers[1*], Christoph Glotzbach[1], Manuel Schmid[1] Katja Tielbörger[2]

[1]Department of Geosciences, University of Tübingen, 72076 Tübingen, Germany

[2]Department of Biology, Plant Ecology Group, University of Tübingen, Auf der Morgenstelle 5, 72076 Tübingen, Germany

Correspondence to: Todd A. Ehlers (todd.ehlers@uni-tuebingen.de)

Abstract. Catchment erosion and sedimentation are influenced by variations in the rates of rock uplift (tectonics), and periodic fluctuations in climate and vegetation cover. ~~In this study we applied the Landlab SPACE landscape evolution modelling approach.~~ This study focuses on quantifying the effects of changing climate and vegetation on erosion and sedimentation over distinct climate-vegetation settings applying the Landlab-SPACE landscape evolution model. As catchment evolution is subjected to tectonic and climate forcings at millennial to million-year time-scales, the simulations are performed for different tectonic scenarios and periodicities in climate-vegetation change. We present a series of generalized experiments that explore the sensitivity of catchment hillslope and fluvial erosion and sedimentation for different rock uplift rates (0.05 mm a^{-1}, 0.1 mm a^{-1}, 0.2 mm a^{-1}) and Milankovitch climate periodicities (23 kyr, 41 kyr and 100 kyr). Model inputs were parameterized for two different climate and vegetation conditions at two sites in the Chilean Coastal Cordillera at ~26°S (arid and sparsely vegetated) and ~33°S (Mediterranean). For each setting, steady state topographies were produced for each uplift rate before introducing periodic variations in precipitation and vegetation cover. Following this, the sensitivity of these landscapes was analysed for 3 Myr in a transient state. Results suggest that regardless of the uplift rate, transients in precipitation and vegetation cover resulted in transients in erosion rates in the direction of change in precipitation and vegetation. While the transients in sedimentation were observed to be in the opposite direction of change in the precipitation and vegetation cover, with phase lags of ~1.5 – 2.5 kyr. These phase lags can be attributed to the changes in plant functional type (PFT) distribution induced by the changes in climatic ~~conditions, which is beyond~~ as well as the ~~scope of this study.~~ regolith production rate. These effects are most pronounced over longer period changes (100 kyr) and higher rock uplift rates (0.2 mm yr^{-1}). This holds true for both vegetation and climate settings considered. Furthermore, transient changes in catchment erosion due to varying vegetation and precipitation were between ~35%-110% of the background (rock uplift) rate and ~~are~~ would be measureable with ~~some~~ commonly used techniques (e.g. sediment flux histories, cosmogenic nuclides). Taken together, we find that vegetation-dependent erosion and sedimentation are influenced by Milankovitch timescale changes in climate, but that these transient changes are superimposed upon tectonically driven rates of rock uplift.

Keywords: vegetation dynamics, climate change, tectonics, landscape evolution modelling, SPACE, Landlab

1 Introduction

The pioneering work of G.K. Gilbert (Gilbert, 1877) highlighted that surface uplift, climate, and biota (amongst other things) jointly influence catchment-scale rates of weathering and erosion. In recent decades a wide range of studies have built upon these concepts and quantified different ways in which climate, tectonics, or vegetation cover influence rates of erosion and sedimentation. For example, recent work highlights that ~~higher~~ denser vegetation ~~and~~ or lower precipitation both decrease erosion (Alonso et al., 2006; Bonnet and Crave, 2003; Huntley et al., 2013; McPhillips et al., 2013; Miller et al., 2013; Perron, 2017; Schaller et al., 2018; Starke et al., 2020; Tucker, 2004). In addition, periodic changes in climate (such as changes driven by Milankovitch timescale orbital variations) have also been recognized as influencing rates of catchment erosion and

38   sedimentation (Braun et al., 2015; Hancock and Anderson, 2002; Hyun et al., 2005; Schaller et al., 2004) although our ability

39   to measure orbital timescale induced erosional changes can be challenging (e.g. Schaller and Ehlers, 2006; Whipple, 2009).

40   Several studies have also documented how the combined effects of either climate and vegetation change, or variable rates of

41   rock uplift and climate change (including glaciation) impact catchment scale processes (Herman et al., 2010; Mishra et al.,

42   2019; Schmid et al., 2018; Tucker, 2004; Yanites and Ehlers, 2012). Taken together, the previous studies have found that the

43   long-term development of topography (such as over million-year time scales) is in many situations sensitive to the tectonic,

44   climate, and vegetation history of the region, and that competing effects of different coeval processes (e.g. climate change and

45   tectonics) exist, but are not well understood.

46   Quantification of climate, vegetation, and tectonic effects on catchment erosion is challenging because these processes are

47   confounded and can, if coupled, have opposing effects on erosion and/or sedimentation. For example, precipitation has both

48   direct (positive) as well as indirect effects on erosion that operate via vegetation cover. Namely, plants require water to grow

49   and survive, vegetation cover is usually positively affected by precipitation both on a global scale (i.e. when comparing biomes

50   across latitudinal gradients) as well as on a regional or local scale (e.g. Huxman et al., 2004; Sala et al., 1988; Zhang et al.,

51   2016). Though vegetation cover is also influenced by temperature, seasonality and many other abiotic factors such as soil type

52   and thickness, the positive relationship of biomass and cover with water availability is rather general. For example, in dry

53   ecosystems such as hot deserts or Mediterranean systems, vegetation cover is primarily limited by water availability and is

54   therefore very low. As precipitation increases, vegetation cover increases rapidly, ~~and~~although water availability can still be

55   the limiting factor as well as other factors ~~become limiting~~ (Breckle, 2002). In temperate systems, where water is abundant

56   and soils are well developed, plant growth is primarily limited by low winter temperatures. Overall, the relationship between

57   precipitation and vegetation cover follows a saturation curve with large sensitivity (e.g. measured as rain use efficiency- RUE)

58   to precipitation in arid to Mediterranean systems and low sensitivity in temperate or tropical systems (Gerten et al., 2008;

59   Huxman et al., 2004; Yang et al., 2008; Knapp et al., 2017).

60   Previous modelling and observational studies have made significant progress in understanding the interactions between surface

61   processes and either climate (Dixon et al., 2009; Routschek et al., 2014; Seybold et al., 2017; Slater and Singer, 2013),

62   vegetation (Acosta et al., 2015; Amundson et al., 2015; Istanbulluoglu and Bras, 2005) or coupled climate-vegetation dynamics

63   (Dosseto et al., 2010; Jeffery et al., 2014; Mishra et al., 2019; Schmid et al., 2018). Over geologic (millennial to million-year)

64   timescales, observational studies of these interactions are impossible (or require proxy data) and numerical modeling

65   approaches provide a means to explore interactions between climate, vegetation, tectonics, and topography. The first

66   observational study of this kind suggested that high MAP (mean annual precipitation) is associated with denser vegetation and

67   hence resulting in lower erosion rates (Langbein and Schumm, 1958). One of the first numerical modeling studies

68   implementing a vegetation-erosion coupling was conducted by Collins et al. (2004). This study was followed by work from

69   Istanbulluoglu and Bras (2006), which quantified the effect of vegetation on landscape relief and drainage formation. More

70   recently, work by Schmid et al. (2018) included the effects of transient climate and vegetation coupled with a landscape

71   evolution model to predict topographic and erosional variations over millennial- to million-year timescales. However, Schmid

72   et al., (2018) presented a simplified approach to consider hillslope and detachment-limited fluvial erosion and only considered

73   a homogeneous substrate. Other studies have documented that sediment or bedrock erosion by rivers is not dominated purely

74   by detachment-limited (Howard, 1994) or transport-limited fluvial erosion (Willgoose et al., 1991). Rather, it often involves a

75   combination of, or transition between, both conditions (e.g., Pelletier, 2012). Given this, treatment of bedrock erosion and

76   sediment transport for mixed bedrock-alluvial streambeds provides a more realistic framework for understanding the influence

77   of climate, vegetation, and tectonic processes on topographic development. Recent work (Shobe et al., 2017) presented an

78   additional component (SPACE) to the Landlab surface process model. SPACE allows for the simulation of mixed detachment-

79 transport limited fluvial processes, including separate layers for bedrock and loose sediment. Finally, the sensitivity of

80 topography to different rock uplift rates in variable climate-vegetation settings has not yet been investigated. The combined

81 interactions of tectonics (rock uplift) and variable climate and vegetation warrant investigation given the significant influence

82 of rock uplift on mean elevation, erosion rates and river channel profiles (Kirby and Whipple, 2012; Turowski et al., 2006)

83 and hillslopes.
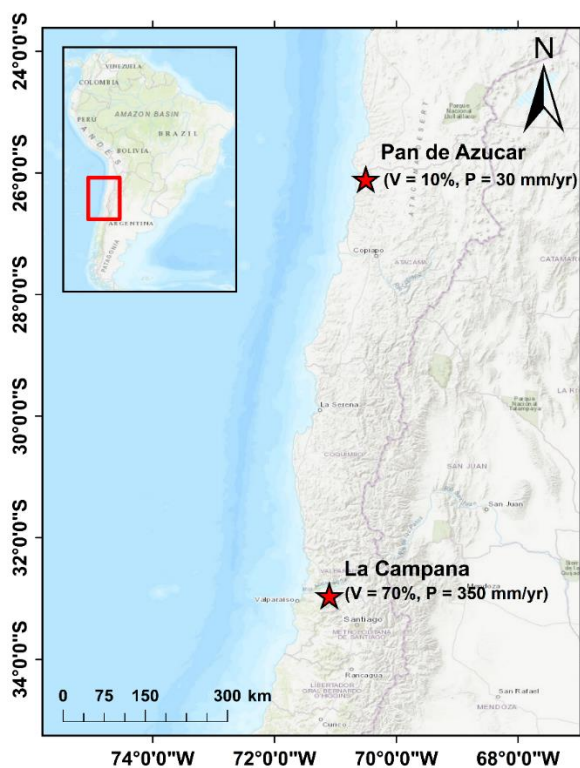
84

85 **Figure 1: The representative study areas in the Chilean Coastal Cordillera used for the model setup. The model parameters were**
86 **loosely tuned to the climate and vegetation conditions in these areas (Schmid et al., 2018). The Pan de Azucar area in the north**
87 **neighbours the Atacama Desert and has sparse vegetation cover (10%) and an arid climate (30 mm yr^{-1}). The La Campana area in**
88 **south has a Mediterranean climate and ecosystem with more abundant vegetation (70%) and precipitation (350 mm yr^{-1}). These two**
89 **study areas are part of the German EarthShape priority research program (www.earthshape.net).**

90 In this study, we complement the previous work and investigate the transient landscape response for mixed bedrock-alluvial

91 systems. We do this for different rates of rock uplift and periodic changes (Milankovitch cycles) in precipitation and vegetation.

92 Our focus is on erosion and sedimentation changes occurring over millennial to million-year timescales. Sub-annual to decadal

93 scale changes are beyond the scope of this study. More specifically, this study evaluates the following two hypotheses: First,

94 if vegetation cover and climate vary on Milankovitch timescales, then any increases or decreases in catchment erosion will be

95 more pronounced over longer (e.g. 100 kyr) rather than shorter (e.g. 21 kyr) periodicities due to the longer duration of change

96 imposed. Second, if increasing rates of tectonic uplift cause increases in catchment erosion rates, then any periodic variations

97 in climate and vegetation cover will be muted (lower amplitude) at higher uplift rates because the effect of rock uplift on

98 erosion will outweigh climate and vegetation change effects. Given the complexity of this problem, we investigate these

99 hypotheses through numerical landscape evolution modelling using a step-wise increase in model complexity where the

100 contributions of individual processes (i.e. climate, or vegetation, or tectonics) are identified separately before looking into the

101 fully coupled system and resulting interactions. We apply a two-dimensional coupled detachment-transport limited landscape

102 evolution model for fluvial processes. In addition, hillslope diffusion (Johnstone and Hilley, 2014) and weathering and soil

103 production (Ahnert, 1977) processes are considered. Although this study is primarily focused on documenting the predicted

104 sensitivity of catchments to variations in tectonics, climate, and vegetation change – we have tuned our model setup to the

105 conditions along the Chilean Coastal Cordillera (Fig. 1) which features a similar tectonic setting, but an extreme climate and

106   ecological gradient. This was done to provide realistic parameterizations for vegetation cover and precipitation in different
107   ecological settings. This area is also part of the German-Chilean priority research program, *EarthShape*: *Earth Surface Shaping*
108   *by Biota* (www.earthshape.net) where extensive ongoing research is occurring.

109   **2 Methods**

110   We apply the landscape evolution model, Landlab (Hobley et al., 2017) using the SPACE 1.0 module of Shobe et al. (2017)

111   for detachment *vs.* transport limited fluvial processes. The Landlab/SPACE programs were modified for vegetation dependent

112   hillslope and fluvial erosion using the approach of Schmid et al. (2018). In general, the geomorphic processes considered

113   involve weathering and regolith production calibrated to the Chilean Coastal Cordillera observations of Schaller et al. (2018),

114   vegetation dependent coupled detachment-transport limited fluvial erosion, and depth dependent hillslope diffusion. The model

115   parameters (i.e., bedrock and sediment erodibility and diffusion coefficient) in the simulations are based on those of Schmid

116   et al. (2018). A detailed explanation of the weathering, erosion, sediment transport and deposition processes is provided in

117   Appendix A, and a summary of model parameters used is given in Table 1.

118   **2.1 Model setup and scenarios considered**

119   The model consists of a 10 km by 10 km rectangular grid with 100 m node spacing (Fig. 2a), with a total domain area of 100

120   km^2. We conducted generalized simulations that are loosely tuned to the climate and vegetation conditions in two areas in

121   the Chilean Coastal Cordillera (Fig. 1) which have predominantly granitoid lithology (van Dongen et al., 2018; Kojima et al.,

122   2017; Oeser et al., 2018; Rossel et al., 2018). These areas exhibit a large climate and vegetation gradient ranging from and

123   arid climate (MAP: 30 mm) and sparse vegetation (10%) in Pan de Azucar National Park to a wetter Mediterranean climate

124   (MAP: 35 cm) with more abundant vegetation (70%) in La Campana National Park.

125   Bedrock elevation and sediment cover thickness are considered as separate layers to quantify simultaneous bedrock erosion

126   and sediment entrainment across the model domain. Simulations were conducted for 15 Myr to generate a steady-state

127   topography with the mean values of precipitation and vegetation cover for the two study areas. The rates of rock uplift are kept

128   constant during the steady-state simulations, and subsequently in the transient stage with oscillating vegetation cover and

129   precipitation. After the development of a steady-state topography, transient forcings in vegetation cover and mean annual

130   precipitation (MAP) (Fig. 2b) were introduced for 3 Myr. Vegetation cover varied by ±10% around the mean value used to

131   develop the steady-state topography. The 10% vegetation cover variation is based on the dynamic vegetation modelling results

132   of Werner et al. (2018) for the Chilean Coastal Cordillera. They found that from the Last Glacial Maximum to present that

133   vegetation cover in the region varied by ~10%. The periodicity of vegetation change varied between simulations (Table 1).

134   Changes in vegetation cover are driven by climatic variations, where MAP has been shown to be much more influential than

135   temperature changes, especially in relatively dry regions (e.g. Mowll et al., 2015) and in grasslands (e.g. Sala et al., 1988).

136   Many previous studies have shown that annual primary production (ANPP) and associated vegetation cover increases linearly

137   (Mowll et al., 2015; Xia et al., 2014) or in an asymptotic manner with MAP (Huxman et al., 2004; Smith et al., 2017; Yang et

138   al., 2008; Zhang et al., 2016; Knapp et al., 2017). These findings are also highly consistent among different approaches such

139   as global (Gerten et al., 2008) or regional (Zhang et al., 2016) models, field and remotely-sensed observations across biomes

140   and among years (Huxman et al., 2004; Xia et al., 2014; Yang et al., 2008), as well as rapid vegetation responses to rainfall

141   manipulation experiments (Smith et al., 2017). An asymptotic relationship appears the more common case, especially when

142   looking at warm and dry ecosystems, i.e. regions up to approx. 600mm MAP (Huxman et al., 2004; Mowll et al., 2015). Here,

143   it has been demonstrated that the sensitivity of ANPP to MAP decreases from more water-limited systems such as deserts to

144   Mediterranean and temperate regions (Huxman et al., 2004; Yang et al., 2008). Namely, the same increase in MAP will yield

145 much larger increases in vegetation cover in dry regions than in wetter ones. To implement these effects, we use an empirical

146 approach based on vegetation-precipitation relationships observed in the Chilean Coastal Cordillera (see Schmid et al. 2018

147 for details) to estimate what mean annual precipitation rates are associated with different vegetation cover amounts (Fig. 2b,

148 2c).
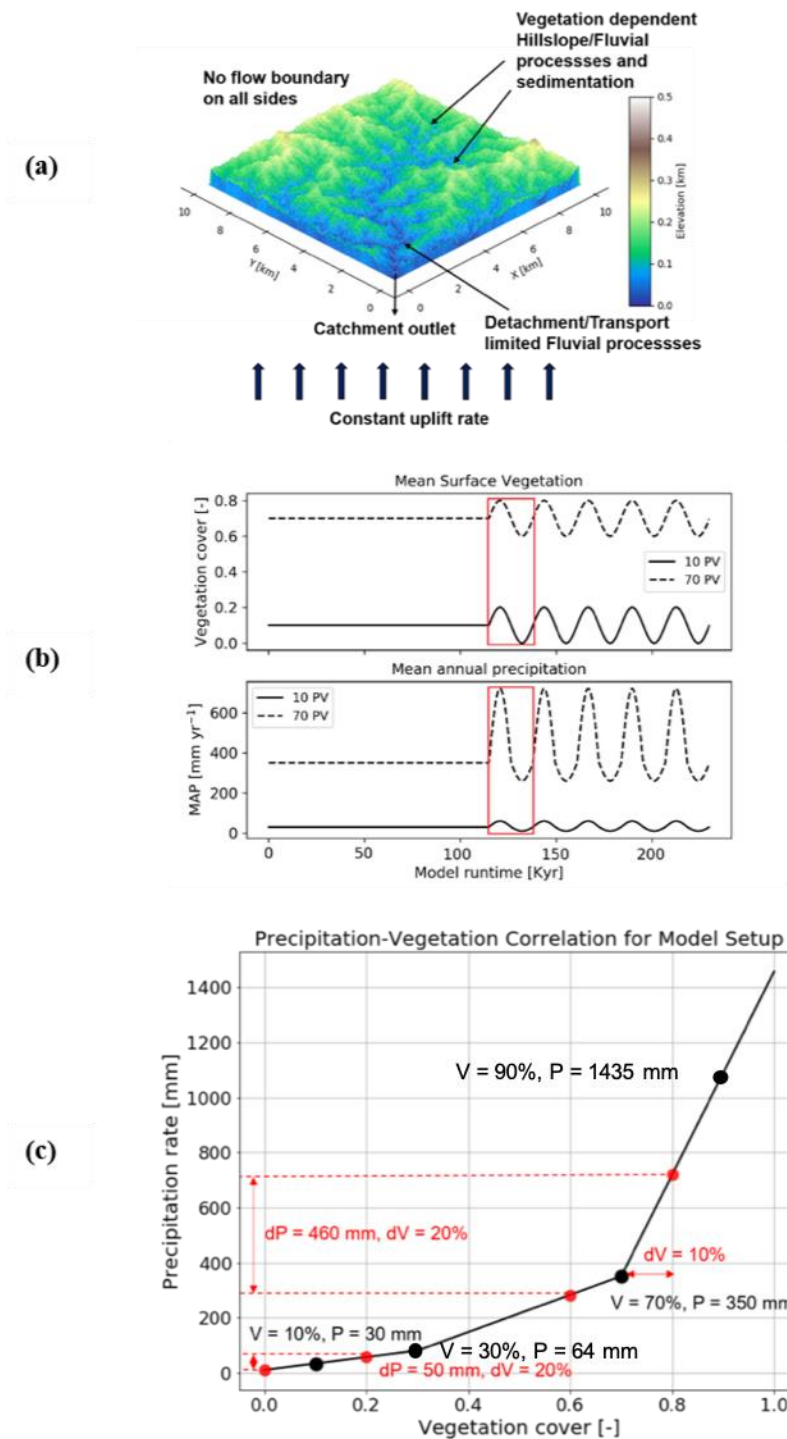
149

150 **Figure 2: Model geometry and climate and vegetation forcings used in this study. (a) A simple representation of the model setup**
151 **with a square grid, and catchment outlet in the lower left corner. (b) Graphical representation of the magnitude and pattern of**
152 **fluctuations imposed on vegetation (top) and precipitation (bottom) during the transient state of the model. Red rectangles represent**
153 **one cycle, whose effects are discussed in detail. (c) Graphical representation of precipitation and vegetation cover correlation from**
154 **the Chilean study areas and used as the empirical bases for how precipitation rates vary for +/-10% changes in vegetation cover**
155 **(Schmid et al., 2018).**

156 The effects of vegetation cover on hillslope and fluvial processes are modified from the approach of Schmid et al, (2018), see

157 also Appendix, and Table 1. Briefly, we applied a slope and depth-dependent linear diffusion rule following the approach of

158 Johnstone and Hilley (2014). The diffusion coefficient (K_d) is defined as a function of the bare soil diffusivity (K_b) and

159 exponentially varies with vegetation cover following the approach of Istanbulluoglu (2005) and Dunne et al. (2010). Fluvial

160 erosion is estimated for a two-layer topography (i.e., bedrock and sediment are treated explicitly) in the coupled detachment –

161 transport limited model. Bedrock erosion and sediment entrainment are calculated simultaneously in the model following the

162 approach of Shobe et al. (2017). The effects of vegetation cover on fluvial erosion were implemented using the approach of

163 Istanbulluoglu (2005) and Schmid et al. (2018) and by introducing the effect of a vegetation dependent Manning's roughness.

164 The sediment and bedrock erodibility (K_{vs} and K_{vr}, respectively) are influenced by the fraction of vegetation cover V (see

165 appendix for governing equations). Figure 3 shows the range of resulting diffusion coefficients (K_d) and sediment and bedrock

166 erodibility (K_{vs}, K_{vb}, respectively) values considered in this study. The exponential and power-law relationships producing

167 these values, respectively, are a source of non-linearity that are manifested in the results discussed in subsequent sections.
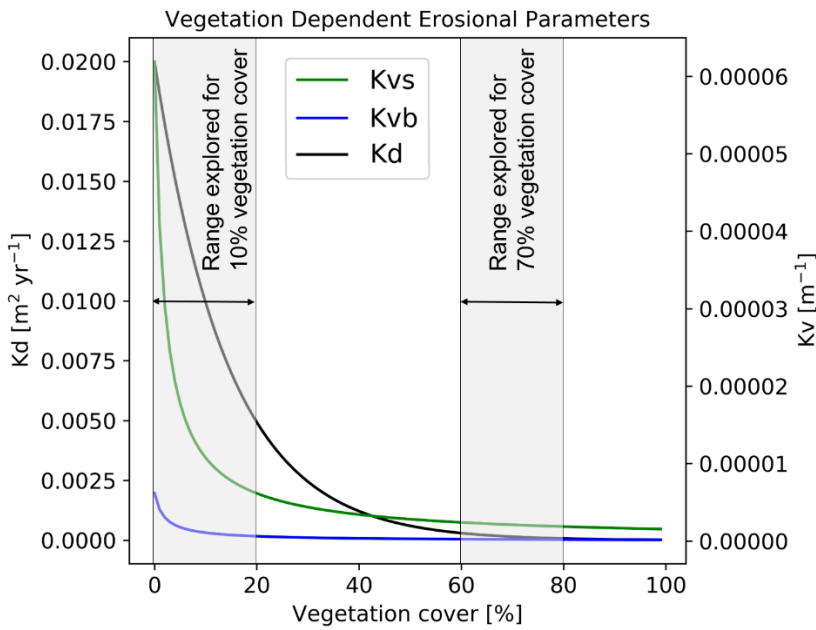
168

169 **Figure 3: Graphical representation of the range of vegetation dependent diffusion coefficient (Kd, left y-axis), sediment erodibility**
170 **(Kvs), and bedrock erodibility (Kvb) values considered in this study (see Appendix for governing equations). The combined**
171 **erodibility is referred to as Kv (right y-axis).**
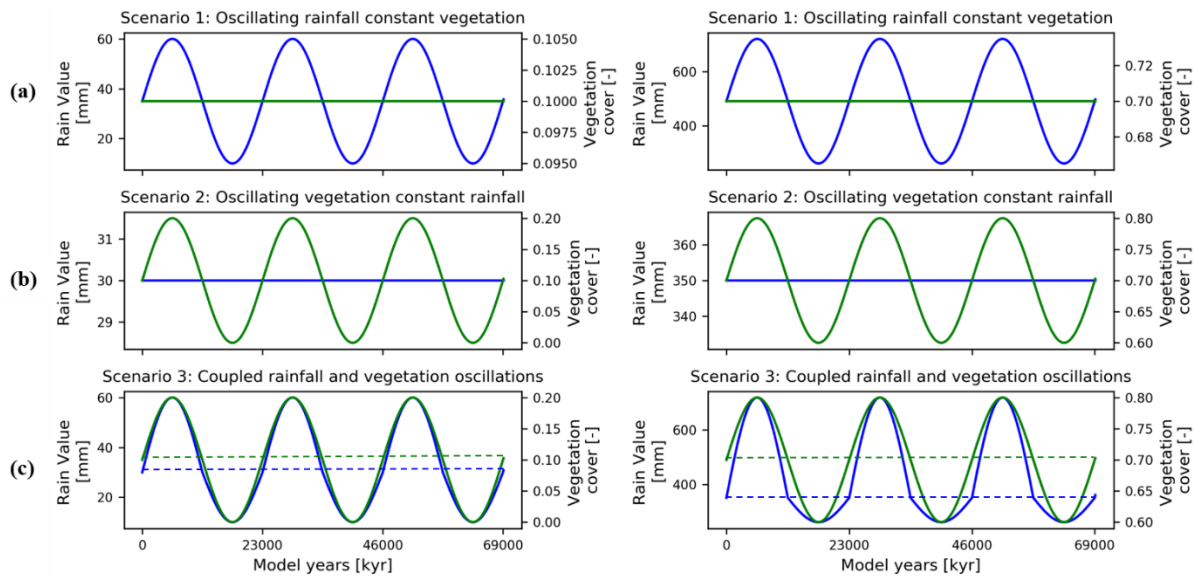
172

173 **Figure 4: Graphical representation of the different precipitation and vegetation forcings applied to the model scenarios described**
174 **in the text. Forcings for sparse vegetation (10%) cover are shown on the left. and dense vegetation (70%) cover on the right. Scenarios**

175 **explored include: (a) Oscillating precipitation and constant vegetation cover. (b) Oscillating vegetation and constant precipitation.**
176 **(c) Coupled oscillations in precipitation and vegetation cover.**

177 As the study areas exhibit similar granitoid lithology, the erosional parameters (Table. 1) are kept uniform for both the study

178 areas. However, parameters based on climate conditions namely soil production rate (Schaller et al., 2018), MAP and

179 vegetation cover (Schmid et al., 2018), are different for these areas. The vegetation cover and precipitation rate are kept uniform

180 across the model domain due to low to moderate relief in target catchments (~750 m for Pan de Azucar and ~1500 m in La

181 Campana).

182 The model scenarios considered were designed to provide a stepwise increase in model complexity to identify how variations

183 in precipitation, vegetation cover, or rock uplift rate influence erosion and sedimentation. The model scenarios include:

184 1. Influence of oscillating precipitation and constant vegetation cover, on erosion and sedimentation (Fig. 4a, Fig. 5, Section
185 3.1).

186 2. Influence of constant precipitation and oscillating vegetation cover, on erosion and sedimentation (Fig. 4b, Fig. 6, Section
187 3.2).

188 3. Influence coupled oscillations in precipitation and vegetation cover, on erosion and sedimentation (Fig. 4c, Fig. 7, Section
189 3.3).

190 4. Influence of different periodicities of precipitation/vegetation change on erosion and sedimentation (Fig. 8, Section 3.4).

191 5. Influence of rock uplift rate and oscillating precipitation/vegetation on erosion sedimentation (Fig. 9, Section 3.5).

192 **Table 1. Landscape evolution model input parameters used and corresponding units.**

Model Parameters	Values
Grid size	10 [km] x 10 [km], dx: 100 [m]
Model runtime (totalTime)	Steady-state: 15 [Ma], Transient state: 3 [Ma]
Rock uplift rates (U)	0.05 [mm a^{-1}], 0.1 [mm a^{-1}], 0.2 [mm a^{-1}]
Periodicities (sinePeriod)	23 [kyr], 41 [kyr], 100 [kyr] (Milankovitch cycles)
Initial sediment thickness (H_initial)	0 [m]
Bedrock erodibility (Kr)	2 x 10^{-9} [m^{-1}]
Sediment erodibility (Ks)	2 x 10^{-8} [m^{-1}]
Soil production/transport decay depth (h*)	0.5 [m]
Reach scale bedrock roughness (H*)	1 [m]
Porosity (φ)	0.2 [-]
Fraction of fine sediments (Ff)	0.2 [-]
Effective terminal settling velocity (Vs)	10 [m a^{-1}]
m, n	0.6, 1 [-]
Bedrock erosion threshold stream power (ω_cr)	5 x 10^{-4} [m a^{-1}]
Sed. entr. threshold stream power (ω_cs)	5 x 10^{-5} [m a^{-1}]
Maximum sediment production rate (W$_o$)	9.7 x 10^{-6} [m yr^{-1}] (10% Veg. cover, 1.3 x 10^{-4} [m yr^{-1}] (70% Veg. cover)
Mean annual precipitation (P)	0.03 [m yr^{-1}] (10% Veg. cover), 0.35 [m yr^{-1}] (70% Veg. cover)
Bare soil diffusivity (K$_b$)	0.01 [m^2 yr^{-1}]
Exponential decay coefficient (α)	0.3 [-]
Critical channel formation area (A$_{crit}$)	1 x 10^6 [m^2]

Reference vegetation cover (V_r)	1 (100%)
Manning's number for bare soil (n_s)	0.01 [-]
Manning's number for ref. vegetation (n_v)	0.6 [-]
Scaling factor for vegetation influence (w)	1 [-]

193 The porosity (0.2) used in this study is lower than usual range for soil (0.3 – 0.4), as sediment produced as a result of weathering

194 in the study areas is a mixture of fine and coarse grained regolith (Schaller et al., 2020). Manning's numbers for bare soil and

195 reference vegetation cover are same as used by Schmid et al., (2018). The rate of rock uplift is kept temporally and spatially

196 constant (0.05 mm a^{-1}) for both study areas, for the simulations in scenarios 1 – 4. This is done in order to minimize the effect

197 of tectonics on topography to isolate the sensitivity of geomorphic processes to changing precipitation and vegetation cover.

198 In scenario 5, the effect of different rock uplift rates (i.e., 0.05 mm a^{-1}, 0.1 mm a^{-1} and, 0.2 mm a^{-1}) is studied in combination

199 with the coupled oscillations in precipitation and vegetation cover. The rock uplift rate used in the scenarios 1 – 4 is influenced

200 by estimated from the findings of Melnick (2016) and Avdievitch et al. (2018), which suggests the modern and paleo uplift

201 and exhumation rates of < 0.1 mm a^{-1} for the study areas and northern Coastal Cordillera in general. Similarly, the periodicity

202 of oscillations for precipitation and vegetation cover are kept constant (23 kyr) for model scenarios 1, 2, 3, and 5. In scenario

203 4, the effect of different periodicities (i.e., 23 kyr, 41kyr, and 100 kyr) is studied in combination with coupled oscillations in

204 precipitation and vegetation cover. The periodicities of oscillations are based on Milankovitch cycles (Ashkenazy et al., 2010;

205 Hyun et al., 2005). In the simulations with variations in either vegetation cover or climate, a perfect sinusoidal function is used

206 to demonstrate the oscillations in precipitation rates for both catchments (Fig. 4a,4b). However, in case of coupled oscillations

207 in vegetation cover and climate, an asymmetric sinusoidal function is used for precipitation rates (Fig. 4c). This is done due to

208 the observed non-linear relationships between changing vegetation cover and precipitation in Figure 2. The non-linearity stems

209 from the fact that in high vegetation cover settings (e.g., 70%, Fig. 2) a large increase in precipitation is needed to increase

210 vegetation cover by 10% compared to a smaller decrease in precipitation required to reduce vegetation cover by 10%.

211 **2.2 Boundary and Initial conditions**

212 An initial low relief (< 1 m) random noise topography was applied to the model grid at the start of the simulations. The initial

213 topographies had a slight initial topographic slope of $\approx 1.4 \times 10^{-5}$ (Fig. 2a). The boundaries on all sides of the domain were

214 closed (no flow), except the south-west corner node which was an outlet node. From these conditions, the steady-state

215 topography was calculated over 15 Myr model time, and the resulting bedrock elevation and sediment thickness were used as

216 input for the transient scenarios described in section 2.1.

217 **3 Results**

218 In the following sections, we focus our analysis on the mean catchment sediment thickness (i.e. the combined thickness of soil

219 and regolith) over the entire domain, mean bedrock erosion rates (excluding sediment erosion), mean sediment entrainment

220 rates and the mean catchment erosion rates. The mean catchment erosion rates are the sum of bedrock erosion and sediment

221 entrainment rates. To simplify the presentation of result, results are shown only for the first cycle of transient climate and

222 vegetation change. Results from the first cycle were representative of subsequent cycles (not shown), and no longer-term

223 variations or trends in erosion/sedimentation were identified or warrant discussion.

3.1 Influence of oscillating precipitation and constant vegetation cover on erosion and sedimentation (Scenario 1)

In this scenario, with a rock uplift rate of 0.05 mm a^{-1} and 23kyr periodicity in precipitation, the mean catchment sediment entrainment rates follow the pattern of change in precipitation (Fig. 5a, b), but with an offset (phase lag) between the maxima and minima of entrainment and precipitation. A higher variation in the range of sediment entrainment rates (i.e., - 0.036 mm yr^{-1} – 0.043 mm yr^{-1}, Fig. 5b) is observed for simulations with 10% vegetation cover. Negative values in sediment entrainment rates corresponds to sediment deposition rates during drier periods. The peak in sediment entrainment rates (e.g. 0.043 mm yr^{-1} for 10% veg., and ~0.038 mm yr^{-1} for 70% veg., Fig. 5b), is observed with a time lag of (~ -2 kyr) before the peak in maximum precipitation in both the 10% and 70% vegetation cover simulations. This result suggests that as precipitation increases sediment is readily entrained where available in the catchment until bedrock is locally exposed. The changes in mean catchment sediment thickness (Fig. 5c) are influenced by changes in the sediment entrainment and precipitation rates, but with a lag time between the maximum in precipitation and the minimum in sediment thickness. The lowest mean catchment sediment thickness (e.g. ~0.97 m for 10% veg., and ~1.9 m for 70% veg., Fig. 5c) also occurs with a time lag of (~3 kyr) after the peak in precipitation rates, for both the 10% and 70% vegetation cover simulations. The same time lag (~3 kyr) is observed in the peak in mean catchment bedrock erosion (e.g. ~0.087 mm yr^{-1} for 10% veg. and ~0.1 mm yr^{-1} for 70% veg., Fig. 5d) and coincides with when the minimum sediment cover is present and more bedrock is exposed for erosion. As we use the total change in bedrock elevation to estimate bedrock erosion rates, the loss in bedrock due to weathering (exponential) is also accounted for. The phase lag in bedrock erosion and sediment thickness can be attributed to exponential weathering, which is discussed in detail in section 4.2. Finally, the mean-catchment erosion rates follow the pattern of change in precipitation rates (Fig. 5a, 5e) without a phase lag. The maximum erosion rates are similar in range for both the 10% and 70% vegetation cover simulations (e.g. ~ 0.12 mm yr^{-1}, Fig. 5e). However, in the 10% vegetation cover simulation, the minimum in the mean catchment erosion rate decreases more (e.g. to ~ 0.01 mm yr^{-1}, Fig. 5e) relative to the higher vegetation cover scenario. The different decreases in the minimum erosion rate between the two vegetation cover amounts corresponds to the differences in precipitation rates (Figs 5a, 4a).

249
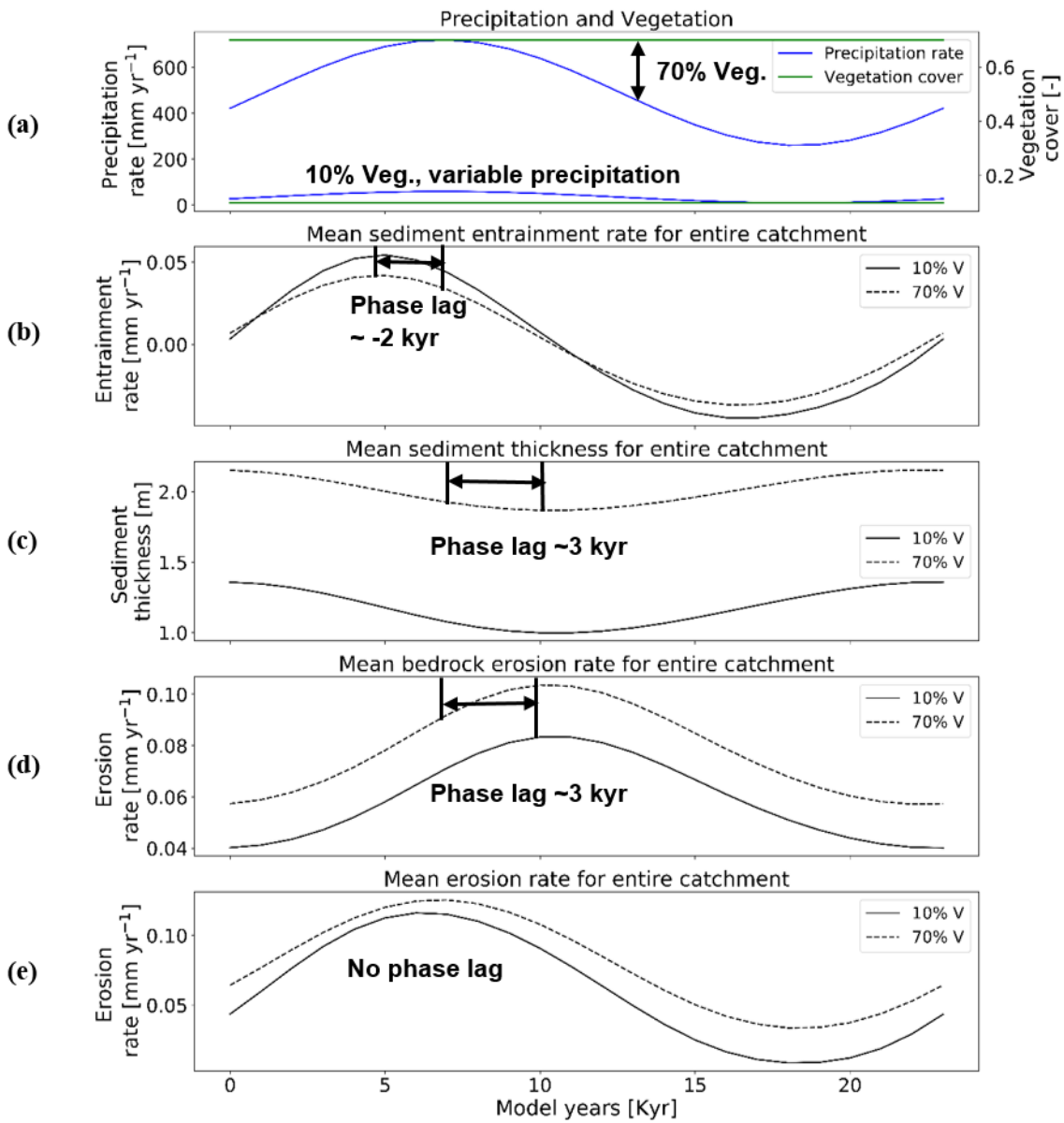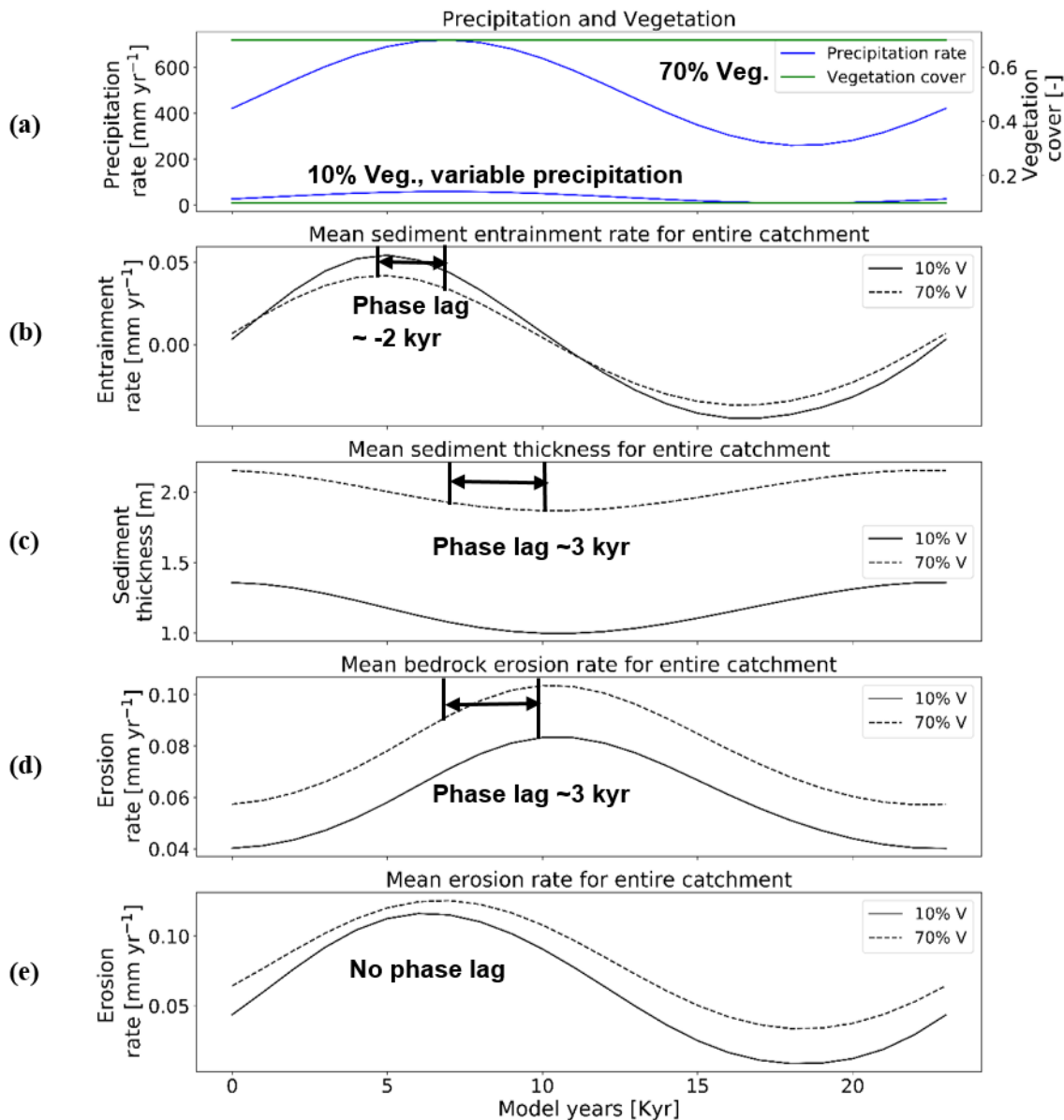
Figure 5: Temporal evolution of catchment averaged predictions for scenario 1 described in the text (section 3.1). Graphical representation of mean catchment sedimentation and erosion to (a) oscillating precipitation [mm yr⁻¹] and constant vegetation cover [-] in terms of ~~(b) sediment entrainment [mm yr-1], (c~~b) sediment thickness [m], (d~~e) bedrock erosion [mm yr-1], ~~(d) sediment entrainment [mm yr-1],~~ (e) mean erosion rates [mm yr⁻¹] for entire catchment. The periodicity of climate and vegetation oscillations is 23 kyr with rate of rock uplift as 0.5 mm yr⁻¹.

The absence of a phase lag between the mean-catchment erosion and precipitation rates reflects that the combined sediment entrainment and bedrock erosion rates when added together track the overall trend in precipitation rate changes, but the individual components (sediment vs. bedrock) respond differently.

3.2 Influence of constant precipitation, oscillating vegetation cover, on erosion and sedimentation (Scenario 2)

Results from this scenario with constant mean annual precipitation (at the mean value of the previous scenario) and oscillating vegetation cover (Fig. 4b. 6a) show a starkly different catchment response from scenario 1 (section 3.1). The sediment entrainment rates show for both simulations (Fig. 6b) a small decrease in entrainment as vegetation cover increases (e.g. ~ -0.05 mm yr⁻¹ for 10% veg., and ~ -0.01 mm yr⁻¹ for 70% veg., Fig. 6b. As vegetation cover decreases later in the cycle, entrainment rates increase (e.g. to ~0.13 mm yr⁻¹ for 10% veg., and to 0.01 mm yr⁻¹ for 70% veg., Fig. 6b). The larger magnitude of increase in entrainment for the 10% vegetation cover case corresponds to the minimum (0%) in vegetation cover where the

265   potential for erosion is the highest. In the 10% vegetation cover simulation, the lowest mean catchment sediment thickness

266   (Fig. 6c was observed ~1.5 kyr after the minimum in vegetation cover (Fig. 6c).

267

268

269
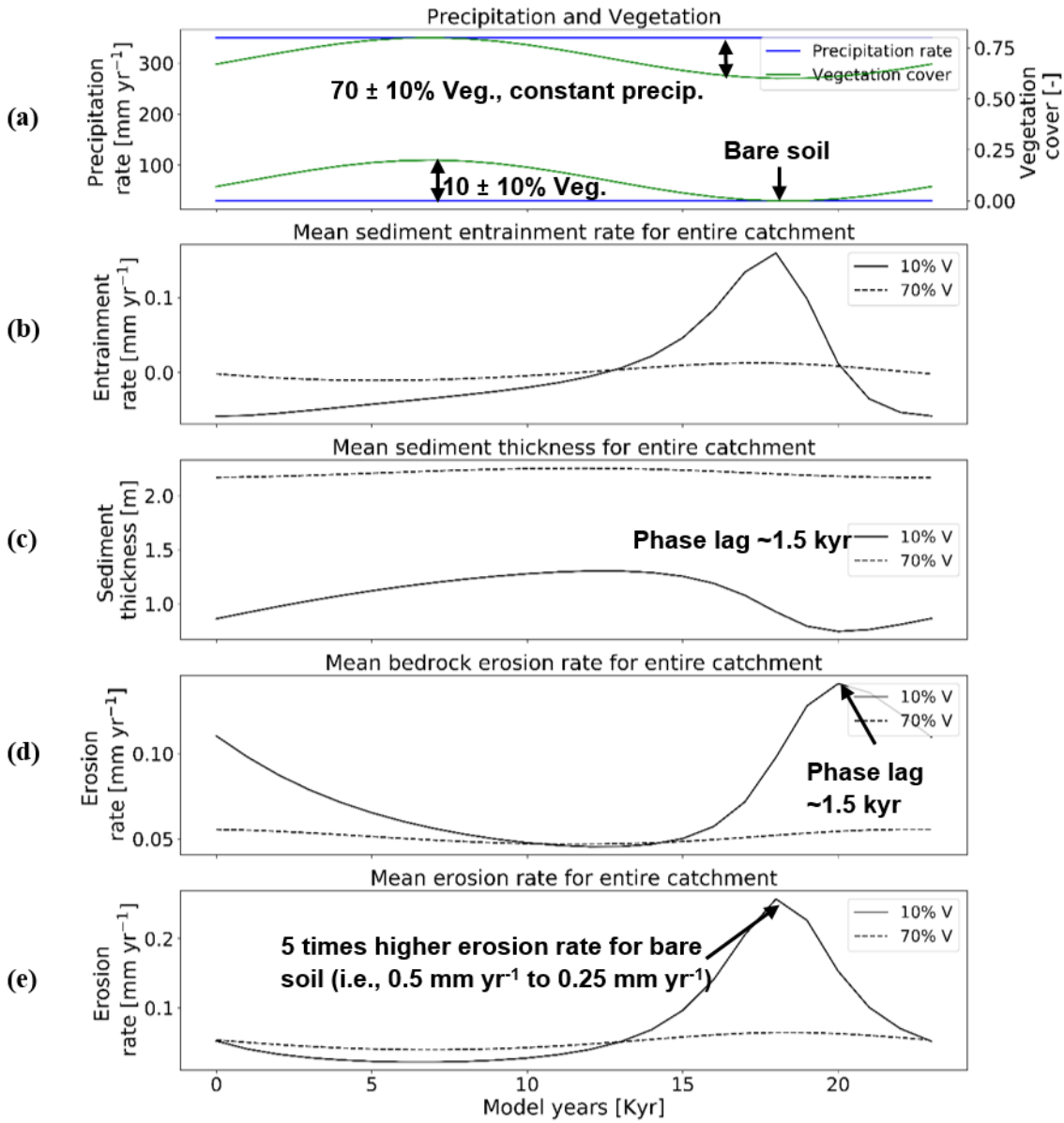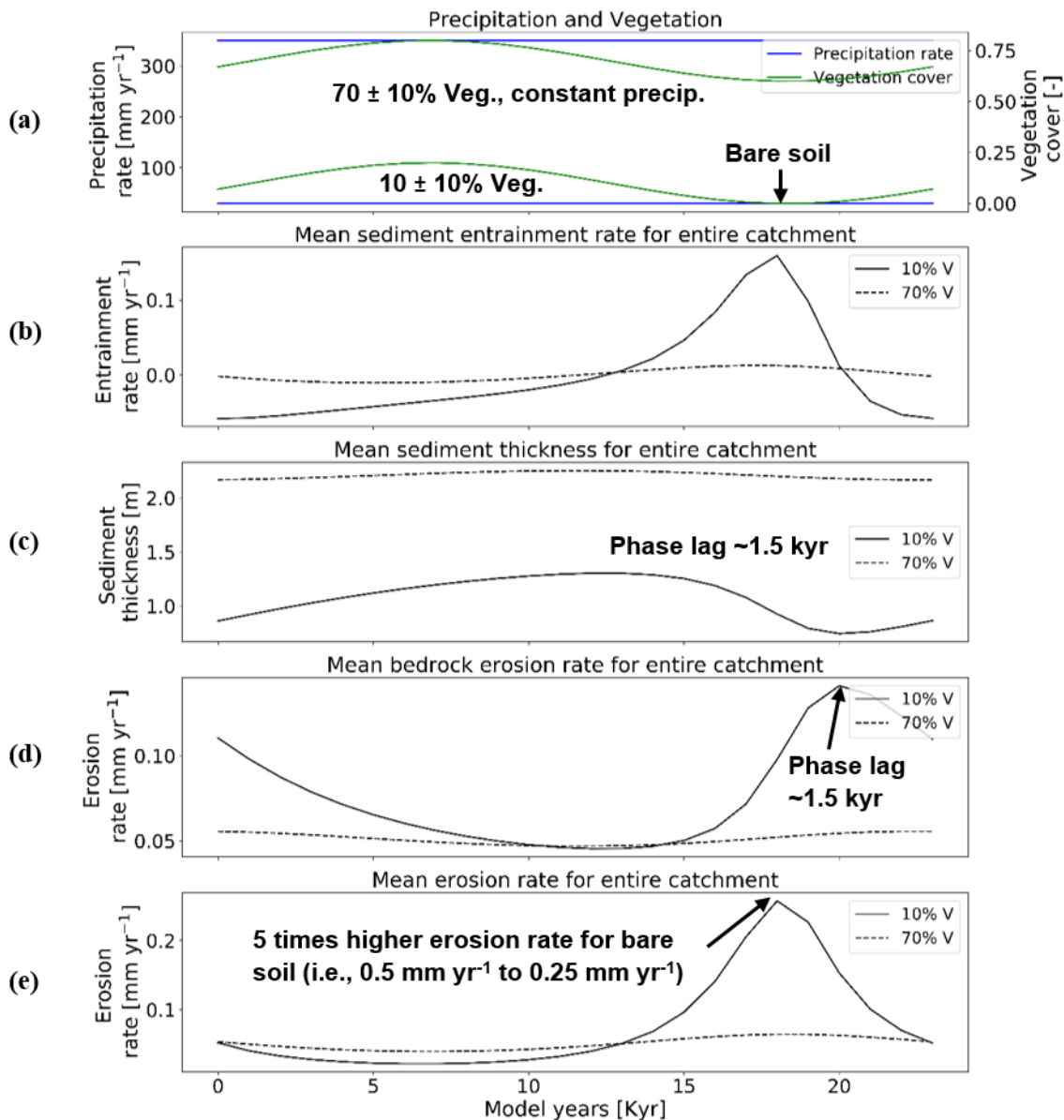
Figure 6: Temporal evolution of catchment averaged predictions for scenario 2 described in the text (section 3.2). Graphical representation of mean catchment sedimentation and erosion to (a) constant precipitation [mm yr⁻¹] and oscillating vegetation cover [-] in terms of (b) sediment entrainment [mm yr⁻¹], (c~~b~~) sediment thickness [m], (d~~e~~) bedrock erosion [mm yr⁻¹], ~~(d) sediment entrainment [mm yr⁻¹],~~ (e) mean erosion rates [mm yr⁻¹] for entire catchment. The periodicity of climate and vegetation oscillations is 23 kyr with rate of rock uplift as 0.5 mm yr⁻¹.

The range of mean catchment sediment thickness varies significantly in the simulations (e.g. ~0.72 m - ~1.38 m for 10% veg., and ~2.2 m – ~2.3 m for 70% veg., Fig. 6c). The same time lag (~1.5 kyr) is observed between the peak in mean catchment bedrock erosion rates (Fig. 6d) and the minimum in vegetation cover. This is most likely due to the maximum exposure of bedrock for erosion when catchment average sediment thicknesses are at their minimum. Also, the first phase of the cycle is mainly depositional while bedrock erosion (including weathering) is observed, which happens partly in places where there is no deposition. Finally, mean catchment erosion rates (Fig. 6e) are significantly affected (~ +0.25 mm yr⁻¹) by oscillating vegetation cover in simulations with a mean 10% vegetation. ~~In the 10% vegetation cover simulation, the maximum in erosion rate occurs during the minimum (0%) in vegetation cover.~~ For the 70% vegetation cover simulation, a similar maximum in erosion occurs also during the minimum in vegetation, but is far less dramatic, presumably due to the still somewhat large (60%) amount of vegetation-cover present. Although the relief and slopes are lower in sparsely vegetated catchment (10% V),

285 significantly higher erosion rates are observed as precipitation is kept constant at 30 mm yr^{-1}, while the vegetation cover was

286 reduced to 0%. This can be attributed to low (bedrock/sediment) stream power thresholds.

3.3 Influence of coupled oscillations of precipitation and vegetation cover, on erosion and sedimentation (Scenario 3)

The catchment response to coupled oscillations in precipitation rate and vegetation cover (Fig. 4c) on erosion and sedimentation represents a composite of the effects discussed in the previous 2 sections (Fig. 7). For example, the mean catchment sediment entrainment rates have a peak in entrainment rates (~1.5 kyr) prior to the peak in climate/vegetation values. A similar effect was noted for scenarios 1 (Fig. 5, section 3.1). As the precipitation rates and vegetation cover decrease later in the cycle (Fig. 7a), the sediment entrainment rates increase. In more detail, the 70% vegetation cover simulations show a modest increase similar to that observed in scenario 1 (Fig. 5b), whereas the 10% vegetation cover shows are sharp peak in the sediment entrainment rates when 0% vegetation cover is present. This later observation is similar what is observed for scenario 2 (Fig. 6b, section 3.2). Thus, in the case of co-varying precipitation rates and vegetation cover, the response observed in terms of sediment entrainment is not predicted to be the same for all degrees of vegetation cover, and depends heavily on the initial vegetation cover of the system around which variations occur.

299
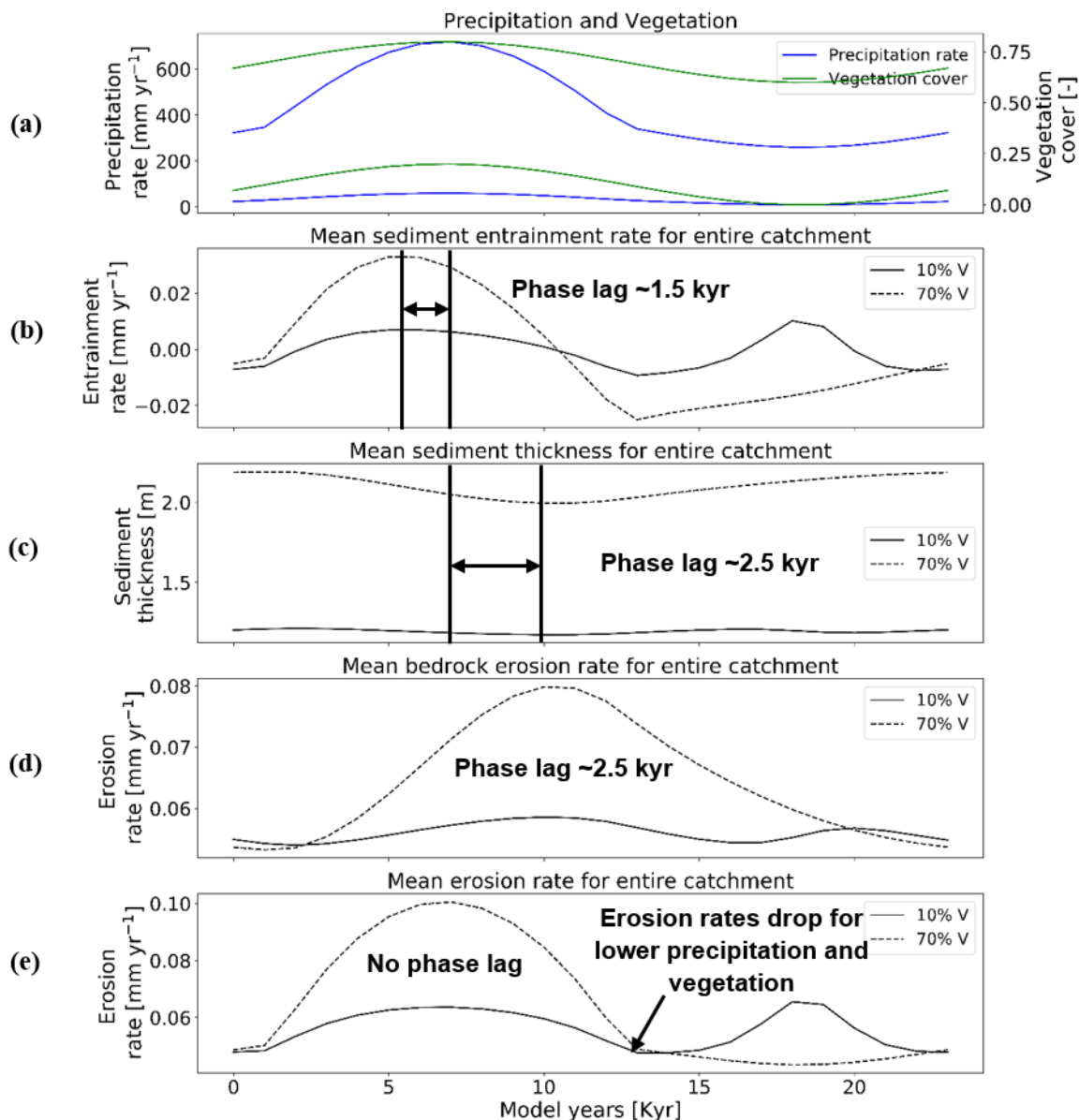
Figure 7: Temporal evolution of catchment averaged predictions for scenario 3 described in the text (section 3.3). Graphical representation of mean catchment sedimentation and erosion to (a) coupled oscillations in precipitation [mm yr⁻¹] and vegetation cover [-] in terms of ~~(b) sediment entrainment [mm yr⁻¹]~~, (c~~b~~) sediment thickness [m], (d~~e~~) bedrock erosion [mm yr⁻¹], ~~(d) sediment entrainment [mm yr⁻¹],~~ (e) mean erosion rates [mm yr⁻¹] for entire catchment. The periodicity of climate and vegetation oscillations is 23 kyr with rate of rock uplift as 0.5 mm yr⁻¹.

Mean catchment sediment thicknesses in the 10% vegetation cover simulation show a modest response and vary between 1.16 m – 1.24 m (Fig. 7c), and with a time lag of ~2.5 kyr between the peak in precipitation/vegetation and minimum sediment thickness. This lag is also observed in the case of the 70% vegetation cover simulation, but with a higher amplitude of change in sediment thickness (e.g. 2 m – 2.22 m, Fig. 7c). A similar trend in time lags between the peaks in climate/vegetation and bedrock erosion (Fig. 6d) are also present. These observations for variations in sediment thickness again represent the combined effects of the results discussed in section 3.1 and 3.2 (Figs. 5c, 6c).

The amplitude of change in bedrock erosion is between 0.05 mm yr⁻¹ – 0.06 mm yr⁻¹ for 10% veg., and 0.05 mm yr⁻¹ – 0.08 mm yr⁻¹ for 70% veg. (Fig. 7d). The bedrock erosion response for both simulations represents a composite of the effects shown in the previous two scenarios (sections 3.1, 3.2). Here the increase in time lag in the maximum in erosion rates (most notable for the 70% vegetation cover simulation) resembles the effect of a large increase in precipitation rates (compared Fig. 5d) for the first part of the cycle. Whereas, the second peak in bedrock erosion visible in the 10% vegetation cover scenario more

closely resembles the effects shown in Fig 6d when the vegetation cover goes to 0%, and the landscape is increasingly sensitive to erosion with whatever runoff (albeit little) is available.

Finally, the mean catchment erosion rates (Fig. 7e) again show the combined effects of the sediment entrainment rate and bedrock erosion histories previously discussed (Figs. 7b, d). In the simulation with 70% initial vegetation cover, the mean catchment erosion rates follow the pattern of changes in precipitation rates (e.g. ranging from 0.04 mm yr^{-1} to 0.1 mm yr^{-1}, Fig. 7e, see also Fig. 5e). A similar trend is present in the first half of the cycle in the simulation with 10% vegetation cover, but with much lower magnitudes (i.e., 0.05 mm yr^{-1} to 0.06 mm yr^{-1}, Fig. 7e). However, during the second half of the cycle, the erosion rates increase up to ~0.06 mm yr^{-1} and have a second peak at ~17-18 kyr for the 10% vegetation simulation when the vegetation cover is at 0%. The previous result is however in contradiction to the detachment-limited results shown in Fig 17 of Schmid et al. (2018), who found that erosion rates decreased to 0 mm yr^{-1} for the period of no vegetation cover and minimum precipitation rate of (~10 mm yr^{-1}). This contradiction is related to the increase in sediment entrainment at this time (Fig. 7b) which heavily influences the mean erosion. The detachment-limited approach of Schmid et al. (2018) could not account for this, and will be discussed in detail in section 4.2. To summarize, as discussed previously the locations of the maximums and minimums in the mean erosion rate and the shape of the curves (Fig. 7e) can be linked to different times in the climate and vegetation history when either the effects of variable precipitation rate or vegetation cover dominate the mean catchment erosional response.

3.4 Influence of the periodicity of precipitation/vegetation variations on erosion and sedimentation (Scenario 4)

Here we show the influence of different periodicities (23, 41, and 100 kyr) in precipitation and vegetation change on catchment erosion and sedimentation for the cases of a 10% mean vegetation cover (Fig. 8) and 70% vegetation cover (Fig. 9). We find higher variations in mean sediment entrainment rates (Fig. 8b, 9b) for both the 10% and 70% vegetation cover simulations for the shorter periodicities (23 and 41 kyr). However, the phase lag in the peaks of sediment entrainment and precipitation rates was higher for longer periodicities (e.g. ~9%, ~16.2%, ~19% in 23 kyr, 43 kyr, and 100 kyr, respectively) for the 10% vegetation cover case (Fig. 8b). These phase lags are however, dampened in the highly vegetated landscapes (70%) at longer periods (i.e., ~9%, ~9.5%, ~14% in 23 kyr, 43 kyr, and 100 kyr respectively, Fig. 9b). In a landscape with 10% vegetation cover, the simulation with longer periodicity (100 kyr) shows higher variations in mean catchment sediment thickness (e.g. 1.14 cm - 1.25 cm, Fig. 8c). This is mimicked in the landscape with 70% vegetation cover, with the range of sediment thickness between 1.95 cm – 2.27 cm (Fig. 9c). A similar trend with higher amplitude of change is also observed for bedrock erosion rates in the sparsely vegetated landscape (10%) with values ranging from 0.05 mm a^{-1} to 0.062 mm yr^{-1} (Fig. 8d) for longer periodicity (100 kyr). The same pattern is observed in highly vegetated landscapes (70%), with the values of bedrock erosion rates ranging from 0.045 mm yr^{-1} to 0.094 mm yr^{-1} (Fig. 9d) for the longer periodicity (100 kyr).

346
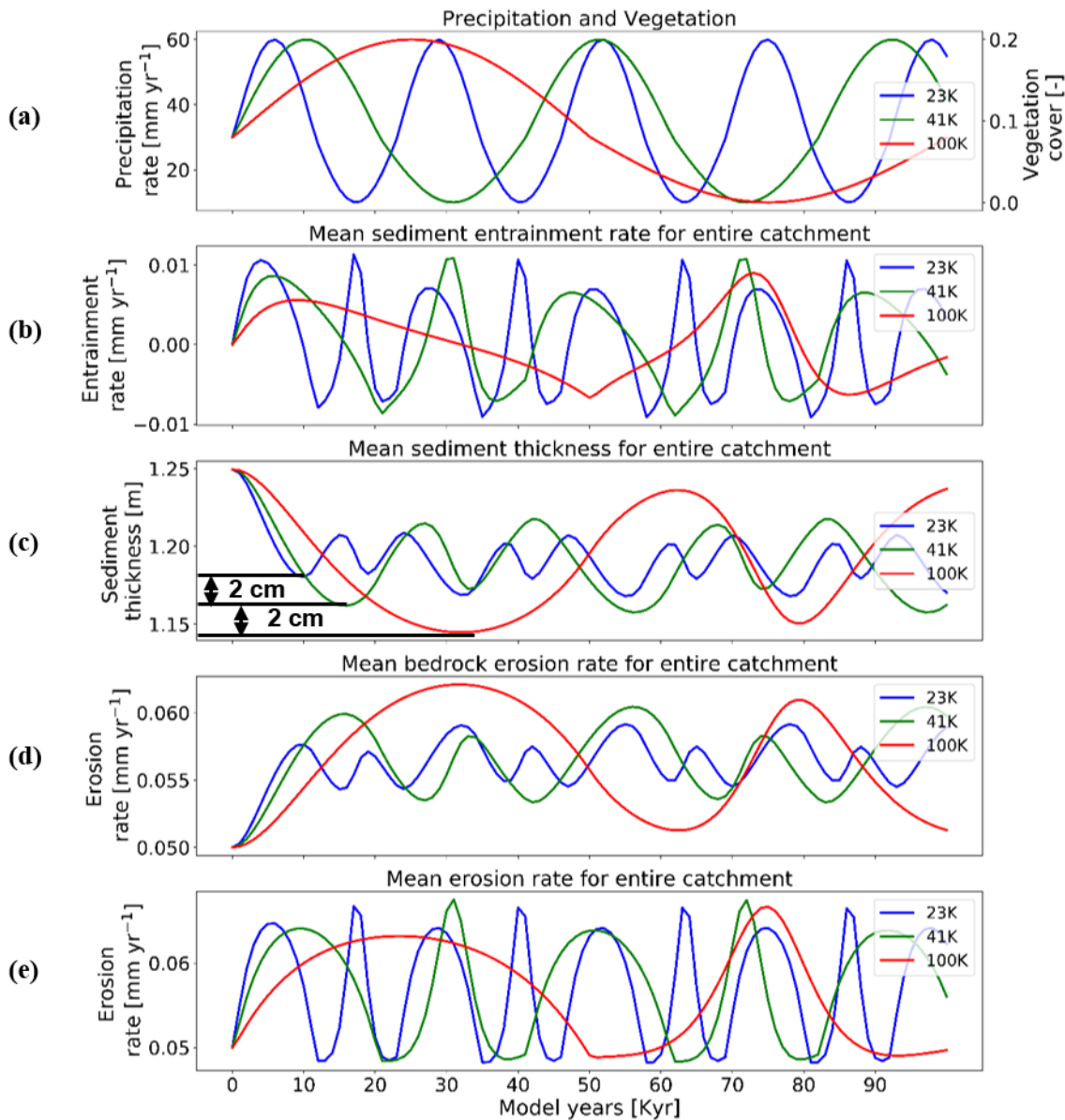
347 **Figure 8: Temporal evolution of catchment averaged predictions for scenario 4 described in the text (section 3.4). Graphical**
348 **representation of mean catchment sedimentation and erosion to (a) different periodicities of coupled oscillations in precipitation**
349 **[mm yr⁻¹] and vegetation cover [-] in terms of (b) sediment entrainment [mm yr⁻¹], (c)** ~~b~~**) sediment thickness [m], (d**~~e~~**) bedrock erosion**
350 **[mm yr⁻¹], ~~(d) sediment entrainment [mm yr⁻¹],~~ (e) mean erosion rates [mm yr⁻¹] for entire catchment. The rate of rock uplift is kept**
351 **constant as 0.5 mm yr⁻¹. The simulations represent 10% initial vegetation cover.**

352

Figure 9: Temporal evolution of catchment averaged predictions for scenario 4 described in the text (section 3.4). Graphical representation of mean catchment sedimentation and erosion to (a) different periodicities of coupled oscillations in precipitation [mm yr⁻¹] and vegetation cover [-] in terms of ~~(b) sediment entrainment [mm yr⁻¹]~~, (c~~b~~) sediment thickness [m], (~~d~~e) bedrock erosion [mm yr⁻¹], ~~(d) sediment entrainment [mm yr⁻¹],~~ (e) mean erosion rates [mm yr⁻¹] for entire catchment. The rate of rock uplift is kept constant as 0.5 mm yr⁻¹. The simulations represent 70% initial vegetation cover.

Overall variations in mean catchment erosion rates (Fig. 8e, 9e) were not observed to be significant (< 0.0001 mm yr⁻¹) as the period of precipitation and vegetation change increases.

3.5 Influence of rock uplift rate and oscillating precipitation/vegetation on erosion sedimentation (Scenario 5)

Here we investigate the response of mean catchment erosion and sedimentation for different rates of rock uplift (i.e., 0.05 mm a⁻¹, 0.1 mm a⁻¹, 0.2 mmyr⁻¹) for the 10% vegetation cover (Fig. 10) and 70% vegetation cover (Fig. 11) scenarios. To simplify the presentation and comparison of results, the periodicity of precipitation and vegetation change is kept the same as section 3.3 (i.e., 23 kyr). In general, the results discussed below demonstrate that the transient catchment response to coupled oscillations in precipitation rate and vegetation cover are similar in shape regardless of the rock uplift rate. The magnitude of change in mean catchment erosion associated with precipitation and vegetation changes increases with increasing uplift rate, despite an identical amount of vegetation and precipitation change imposed (Figs. 10a, 11a) on each rock uplift rate simulation.
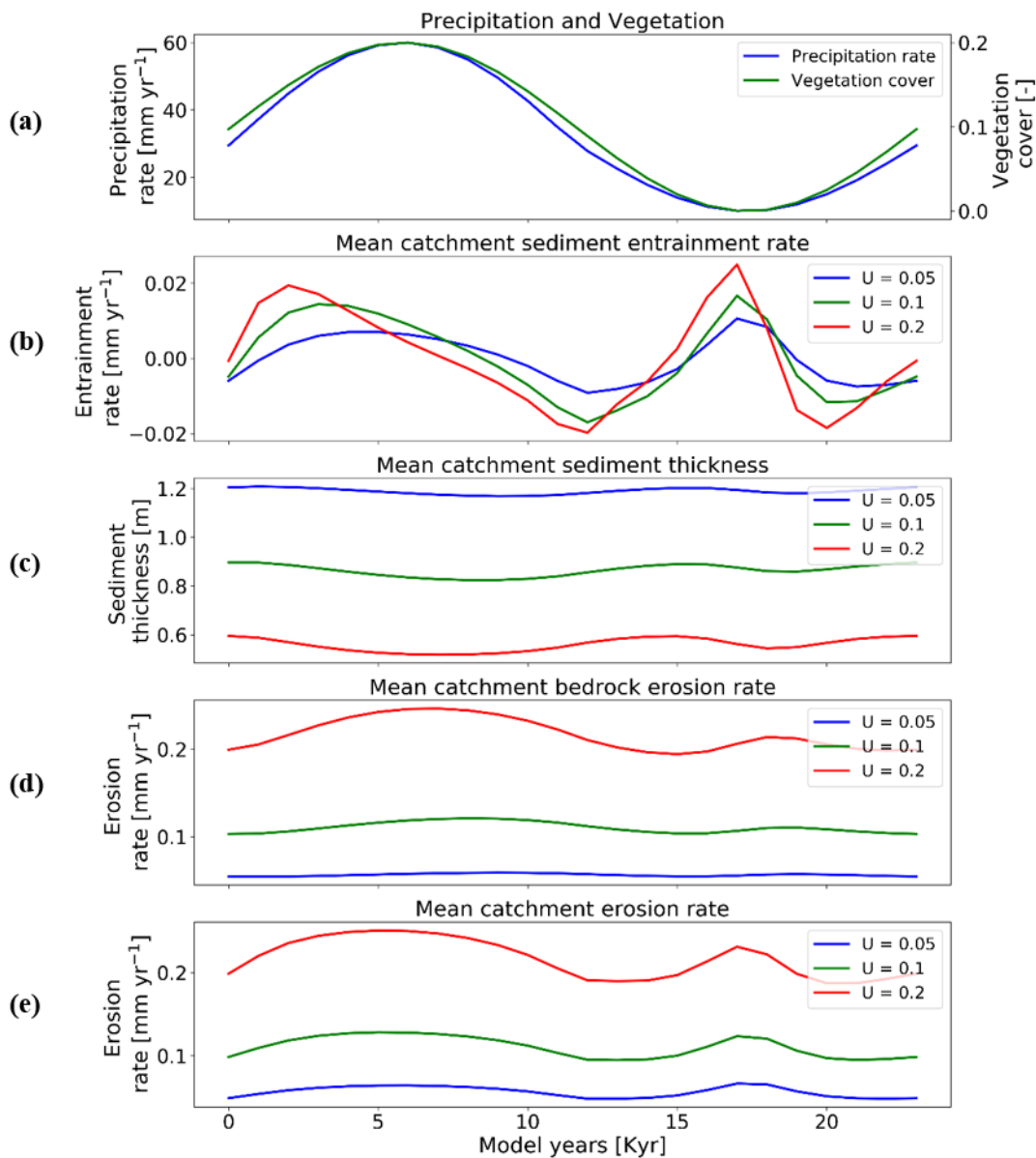
368

369 **Figure 10: Temporal evolution of catchment averaged predictions for scenario 5 described in the text (section 3.5). Graphical**
370 **representation of mean catchment sedimentation and erosion with different rates of rock uplift [mm a⁻¹] to (a) coupled oscillations**
371 **in precipitation [mm yr⁻¹] and vegetation cover [-] in terms of (b) sediment entrainment [mm yr⁻¹], (cb) sediment thickness [m], (de)**
372 **bedrock erosion [mm yr⁻¹], ~~(d) sediment entrainment [mm yr⁻¹],~~ (e) mean erosion rates [mm yr⁻¹] for entire catchment. The**
373 **periodicity of climate and vegetation oscillations is 23 kyr. The simulations represent 10% initial vegetation cover.**
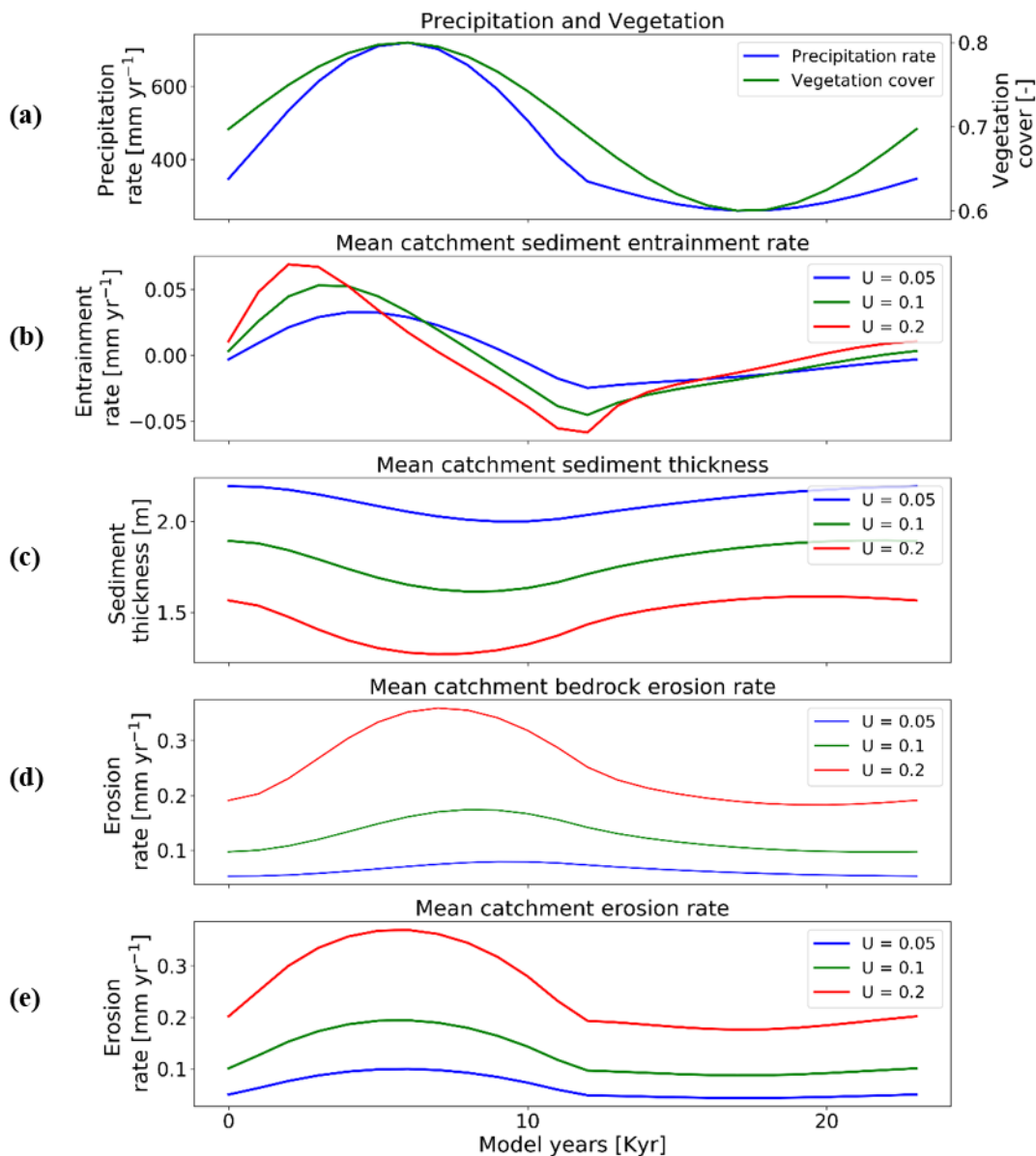
374

375 **Figure 11: Temporal evolution of catchment averaged predictions for scenario 5 described in the text (section 3.5). Graphical**
376 **representation of mean catchment sedimentation and erosion with different rates of rock uplift [mm a⁻¹] to (a) coupled oscillations**
377 **in precipitation [mm yr⁻¹] and vegetation cover [-] in terms of ~~(b) sediment entrainment [mm yr⁻¹]~~, (c~~b~~) sediment thickness [m], (d~~e~~)**
378 **bedrock erosion [mm yr⁻¹], ~~(d) sediment entrainment [mm yr⁻¹],~~ (e) mean erosion rates [mm yr⁻¹] for entire catchment. The**
379 **periodicity of climate and vegetation oscillations is 23 kyr. The simulations represent 70% initial vegetation cover.**

380 In more detail, the temporal pattern of changes in sediment entrainment rates (Fig. 10b, 11b) is similar for all uplift rates

381 considered, but the amplitude of change increases as the uplift rate increases. In addition, the phase lag between the peaks in

382 sediment entrainment rates and maximum precipitation rates in the 10% vegetation simulation (Fig. 10b) varies with the rock

383 uplift rate. ~~The~~ For example, the peaks in sediment entrainment rates ~~are higher for lower rock uplift rates (e.g.~~ have phase lag

384 of ~ -4 kyr, -2.5 kyr, and -2 kyr~~) before the maximum in precipitation~~ for rock uplift rates of 0.2 mm a⁻¹, 0.1 mm a⁻¹, and 0.05

385 mm a⁻¹ respectively (Fig. 10b) in first half of the vegetation/precipitation oscillation. However, the phase lags are overall

386 shorter in highly vegetated landscapes (70%) (e.g. ~ -3 kyr, -2 kyr, -1 kyr) before the maximum in precipitation for rock uplift

387 rates of 0.2 mm a⁻¹, 0.1 mm a⁻¹, and 0.05 mm a⁻¹ respectively (Fig. 11b).

388 For the landscape with 10% vegetation cover, the simulation with the highest rates of rock uplift (0.02 mm a⁻¹) showed lower

389 mean catchment sediment thickness (e.g. ~0.5 m – ~0.6 m, Fig. 10c). In contrast, the slowest rock uplift simulation (0.05 mm

390 a⁻¹) had thicker sediment thickness of ~1.16 m – ~1.24 m, (Fig. 10c). The same pattern was observed in the catchment with

391   70% vegetation cover, where the higher sediment thicknesses occur for the lower rates of rock uplift (e.g. ~2 m - ~2.2 m, Fig.

392   11c). These results for sediment thickness variations reflect that higher rock uplift rates result in steeper slopes (not shown)

393   and higher mean catchment erosion rates (Figs. 10e, 11e) such that regolith production rates are outpaced by erosion and

394   therefore result in thinner sediment thicknesses. Also, the thicker sediment thickness for lower uplift rates could be an

395   integrated result of slightly lower erosion rates compared to sediment production rates over the whole 15 Myr model runtime

396   (steady state). This result is akin to the observational results from Heimsath et al. (1997).

397   Temporal variations in bedrock and mean catchment erosion rates are similar to those described in section 3.3 (Fig. 7) for the

398   sparsely and more heavily vegetated conditions. The primary difference is that at high rock uplift rates the amplitude of

399   bedrock or mean catchment erosion increases (Figs. 10d,e; 11d,e). To summarize, these results highlight that regardless of the

400   rock uplift rate, similar temporal changes are observed in sediment entrainment or thickness, and in bedrock and catchment

401   erosion for oscillating precipitation rates and vegetation cover. However, the amplitude of change (or absolute change) in

402   entrainment and erosion rates increases with increases in rock uplift rate. This will be discussed in detail in section 4.4.

403   **4 Discussion**

404   In this section, we synthesize the results from previous section (scenarios 1-5) in detail. We further investigate the effects of

405   coupled climate and vegetation oscillations (Scenario 3) on the occurrence of erosion and sedimentation on spatial scale.

406   **4.1 Differences in effects between oscillating vegetation or precipitation**

407   Here the sensitivity of erosion and sedimentation to variable precipitation and/or vegetation cover is analysed. In the scenario

408   with oscillating precipitation and constant vegetation cover, sparsely vegetated landscapes (10%) are eroding slowly during

409   periods of lower precipitation. This might be attributed to the dependency of the bedrock erosion and sediment entrainment on

410   the amount of water available through precipitation, which in turn affects the erosion rates. The mean erosion in this scenario

411   is dominated by bedrock erosion with a significant contribution from sediment entrainment. Also, the mean erosion rates over

412   one climate oscillation cycle are observed to be slightly higher (~20%) than mean erosion rates at steady state for sparsely

413   vegetated landscape (10% V). For densely vegetated landscape (70% V), this difference is significant (i.e., 50% higher mean

414   erosion rates during a transient cycle, in comparison to steady state). This implies the non-linearity of the erosion response to

415   changes in MAP, which is significantly higher in densely vegetated landscape where amplitude of change in MAP (e.g., 260

416   mm – 720 mm) is much higher than drier landscapes (e.g., 10 mm – 60 mm).

417   Similarly, in a scenario with constant precipitation and variable vegetation cover, sparsely vegetated landscapes (10%) are

418   observed to be much more sensitive in terms of erosion rates during periods of no vegetation cover. The amplitude of erosional

419   change was ten times higher than that of densely vegetated landscapes. The mean erosion in sparsely vegetated landscapes is

420   dominated equally by bedrock erosion (Fig. 6d) and sediment entrainment, due to the higher availability of bare soil. This

421   justifies the argument of a higher sensitivity of sparsely vegetated landscapes to erosion and sedimentation. This result confirms

422   the findings of Yetemen et al. (2015) (see Fig. 2g), which suggests that shear stress (erosion) decreases significantly (1 to 0.1)

423   as the total grass cover (vegetation) is increased from 0% (bare soil) to 20% grass cover. Also, a small change in vegetation

424   cover in densely vegetated landscapes would not result in significant differences in erosional processes. Unlike previous

425   scenario (oscillating precipitation and constant vegetation cover), we do not observe non-linearity in erosion response to the

426   changes in vegetation cover (i.e., mean erosion rates over one transient cycle are equal to steady state mean erosion rates).

427   In general, mean catchment sediment thickness is observed to be inversely proportional to precipitation, owing to higher stream

428   power. This in turn translates to a higher sediment flux during wetter periods. The influence of oscillating precipitation and

429   constant vegetation cover on sediment thickness is slightly higher in simulations with sparse vegetation cover. In simulations

with constant precipitation and oscillating vegetation cover, the sensitivity of sediment thickness is much higher in landscapes with sparse vegetation. This can be attributed to an absence of vegetation cover. A decreased impact of oscillating vegetation cover on sediment thickness occurs in landscapes with denser vegetation cover and demonstrates that surface processes in these settings are not highly dependent on changes in vegetation density. This has been explained by Huxman et al. (2004), who found that vegetation cover responds to MAP variations in wet and dry systems during dry years.

4.2 Synthesis of coupled oscillations of precipitation and vegetation cover simulations

The sensitivity of erosion and sedimentation to coupled oscillations in precipitation and vegetation cover (scenario 3, section 3.3) indicates that mean catchment erosion rates (Fig. 7e) are correlated with precipitation for densely vegetated landscapes (70%). This is owed to the dominating effect of mean annual precipitation changes (from 26 cm yr^{-1} to 72 cm yr^{-1}) on erosion over vegetation cover change (from 60% to 80%, Fig. 7a) in these landscapes. This can be attributed to the higher amplitude of precipitation oscillations in these simulations required to change vegetation cover by +/-10% (Fig. 2b). In the case of a sparsely vegetated landscape (10%), mean erosion rates (Fig. 7e) are also correlated to precipitation, but only for the first half of the cycle when vegetation cover is present. However, mean erosion rates increase rapidly in the second half of the cycle when MAP decreases (from 60 mm yr^{-1} to 10 mm yr^{-1}, Fig. 7a), and vegetation cover magnitudes decrease (from 20% to 0%, Fig. 7a). This inverse correlation between precipitation and erosion can be attributed to increasing susceptibility of the surface to sediment entrainment as vegetation cover decreases to bare soil, even with very low precipitation rates. The non-linearity of erosion response to changes in MAP is reduced by half (in comparison to changing climate and constant vegetation) in coupled simulations.

Thus, the temporal evolution of mean erosion rates between the heavily (70%) and sparsely (10%) vegetated landscapes varies depending on the initial vegetation state of the catchment. As a result, correlated and anti-correlated relationships between precipitation, vegetation cover, and erosion are predicted and are the result of precipitation or vegetation exerting a dominant or subsidiary influence on catchment erosion at different times in the catchment history and for different catchment precipitation and vegetation cover conditions. This prediction is consistent with observed correlations of vegetation cover and catchment average erosion rates recently documented along the western Andean margin by Starke et al. (2020).

The lag behavior observed in sediment entrainment, thickness and bedrock erosion is explained in additional simulations we conducted (results not shown for brevity) where the weathering (regolith production) function was turned off in the model simulations (see Fig. A1 in appendix). In these simulations, we did not observe any significant phase lags in maximum and minimum of erosion rates, sediment thickness and vegetation cover/precipitation. Also, the erosion rates for sparsely vegetated catchment (10% V), drops to a minimum during the phase of bare soil and minimum precipitation (10 mm yr^{-1}). Hence, sediment supply through weathering can be attributed to double peaks observed in mean catchment sediment entrainment rates (Fig. 7b) and erosion rates (7e). When there is no explicit weathering / regolith production involved in the model simulations, sediment supply for entrainment is significantly reduced. As a result, entrainment rates are observed to be two orders of magnitude lower than bedrock erosion, hence entrainment rates are not shown in Fig. A1. This implies that weathering plays a major role in leading to the phase lags observed in above results.

4.3 Differences between the periodicities of climate and vegetation cover oscillations

The periodicity of change in climate will mainly affect vegetation via the lag-time it takes for the vegetation to respond i.e., if the vegetation structure does not change (e.g., grasslands or forests), then grasslands are very flexible (Bellard et al., 2012; Kelly and Goulden, 2008; Smith et al., 2017). Grasslands can plastically respond from year to year while forests may die off

468 and be replaced by grasslands when it becomes drier and vice-versa. This change in vegetation type might lead to the
469 fluctuations in sedimentation and erosion rates due to periodicity of change in climate and vegetation cover.

4.4 The effect of rock uplift rate on signals of varying precipitation and vegetation cover

471 No difference in erosion rates was identified between the two different vegetation/precipitation simulations for a given uplift
472 rate when the erosion rate is averaged over the full period of vegetation/precipitation change. In a steady state landscape,
473 erosion rates are equal to the rock uplift rates according to the law of continuity of mass (e.g., Tucker et al., 2001). This means
474 that steady state landscapes experience higher erosion rates with higher uplift rates. However, the mean catchment erosion
475 rates shown in Fig. 10e, 11e show temporal variations in the erosion rate driven by oscillations in the precipitation rate and
476 vegetation. When average erosion rates are calculated over a complete cycle of the oscillation, the mean erosion rates are
477 slightly higher than equals the rock uplift rates, owing to the non-linearity of erosion response to changes in MAP. This result
478 indicates that any climate or vegetation driven changes ins erosion will not be evident when observed over too long a period
479 time, but might introduce shorter-term transients (high or low) depending on the climate/vegetation cycle of change. This
480 finding is significant for observational studies seeking to measure the predictions shown in this study. More specifically,
481 thermochronometer dating approaches used to quantify denudation rates over million-year timescales will be hard pressed to
482 measure any signal of how climate or vegetation change on Milankovitch timescales influence denudation. Rather, the rate of
483 tectonic rock uplift or exhumation (in the case of erosion rates equalling the rock uplift rate) will be measured. In contrast,
484 observational techniques sensitive to decadal (e.g. sediment fluxes) or millennial (e.g. cosmogenic radio nuclides measured
485 from river terraces) can be sensitive to timescales less than the period of oscillation and are more like to record transient
486 catchment erosion rates influenced by variations in precipitation or vegetation cover.

487 The vegetation and precipitation driven transients in mean catchment erosion rates predicted by this study were large enough
488 to be measured by some observational techniques. For example, in sparsely vegetated landscapes the half amplitude of change
489 in erosion rates (from steady-state values) slightly decreases as the uplift rate increases. A higher magnitude of change in
490 transient erosion rates (from stead-state values) is found in densely vegetated landscapes and is again slightly decreased as the
491 uplift rate increases. Previous work by Schaller and Ehlers (2006) investigated the ability of denudation rates calculated from
492 cosmogenic radionuclides measured in a sequence of fluvial terraces to record periodic (Milankovitch timescale) variations in
493 denudation rates. The magnitude of change in predicted transient erosion rates described above is above the detection limit
494 reported by Schaller and Ehlers (2006), particularly when the mean catchment denudation rate is ~0.1 mm yr^{-1} or higher. Thus,
495 the predictions suggested in this study are testable in field-based studies, and other methods such as basin sedimentation rate
496 histories (e.g. determined from magneto-stratigraphy, optically stimulated luminescence, or other methods) also hold potential.

4.5 Spatial changes in where erosion and sedimentation changes occur

498 In the previous sections, our analysis focused on the spatially averaged response of the catchment in terms of changes in
499 sedimentation and erosion. Here, we discuss the same model results as previously presented for but show two examples (for
500 two different vegetation covers) of the spatial variations of erosion and sediment thickness within the catchments. This provides
501 a basis for understanding where in the catchment changes are occurring.

502
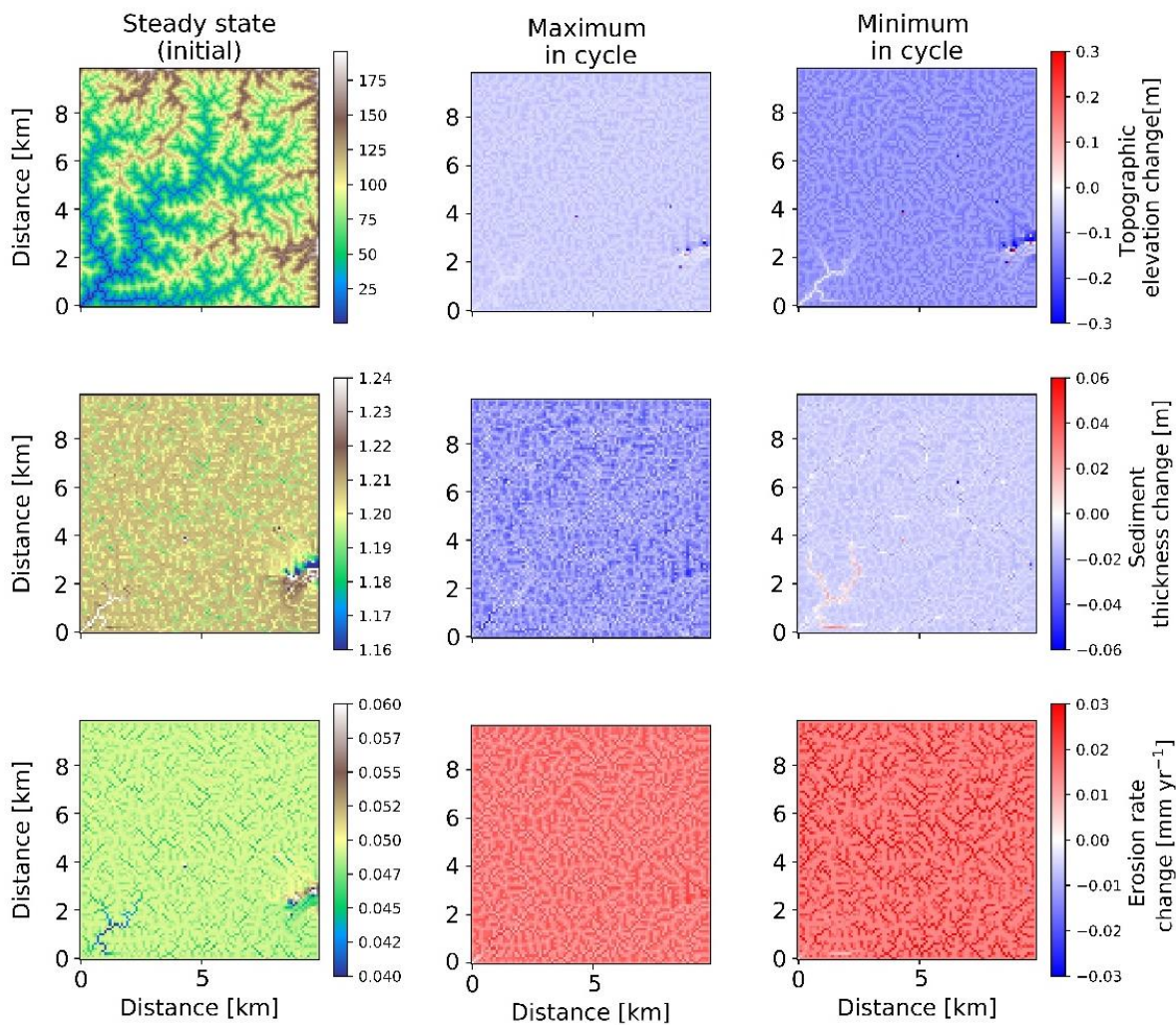
Figure 12: Two-dimensional map-view representation of changes in topographic elevations [m] (1st row), sediment thickness [m] (2nd row), and erosion rates [mm yr⁻¹] (3rd row). These changes are represented with respect to steady state conditions (1st column), for maximum (2nd column) and minimum (3rd column) values of precipitation and vegetation in an oscillation cycle. The simulations represent 10% initial vegetation cover.

Spatial variations in the pattern of erosion and sedimentation in the simulations with 23 kyr coupled precipitation and vegetation oscillations, and a rock uplift rate of 0.05 mm a⁻¹, are shown in the topographic elevation, sediment thickness, and erosion rate changes for both the maximum and minimum in precipitation and vegetation cover. In the simulations with sparse vegetation cover (10%) (Fig. 12) at the maximum in precipitation and vegetation cover, erosion rate changes from steady state are ~0.03 mm yr⁻¹ in valleys and ~0.01 mm yr⁻¹ on hillslopes. At the minimum in precipitation and vegetation cover, erosion rate changes from steady state are higher in valleys than hillslopes. This may be attributed to an absence of vegetation during this period, where the surface (bedrock or sediment) is readily available for erosion even with lower precipitation rates. The sediment thickness is observed to be slightly higher in the streambeds and valleys for streams with larger accumulation area. However, the smaller streams have lower sediment thickness compared to connected hillslopes. For example, higher sediment thickness (~1.24 m) is observed near the catchment outlet in the lower-left corner of the domain. At the maximum in precipitation and vegetation cover cycle, the landscape experiences a slightly higher contrast in sediment thickness compared to the steady-state condition, whereby a net lowering of the sediment layer is observed of approximately 2 cm to 5 cm on the hillslopes and ~6 cm near the catchment outlet. This can be attributed to higher sediment fluxes during this period. At the minimum in the precipitation and vegetation cover cycle, the landscape experiences a slight difference from the steady state sediment thickness (~2 cm lowering) except for deposition in higher order streams (up to ~2 cm) near the catchment outlet.
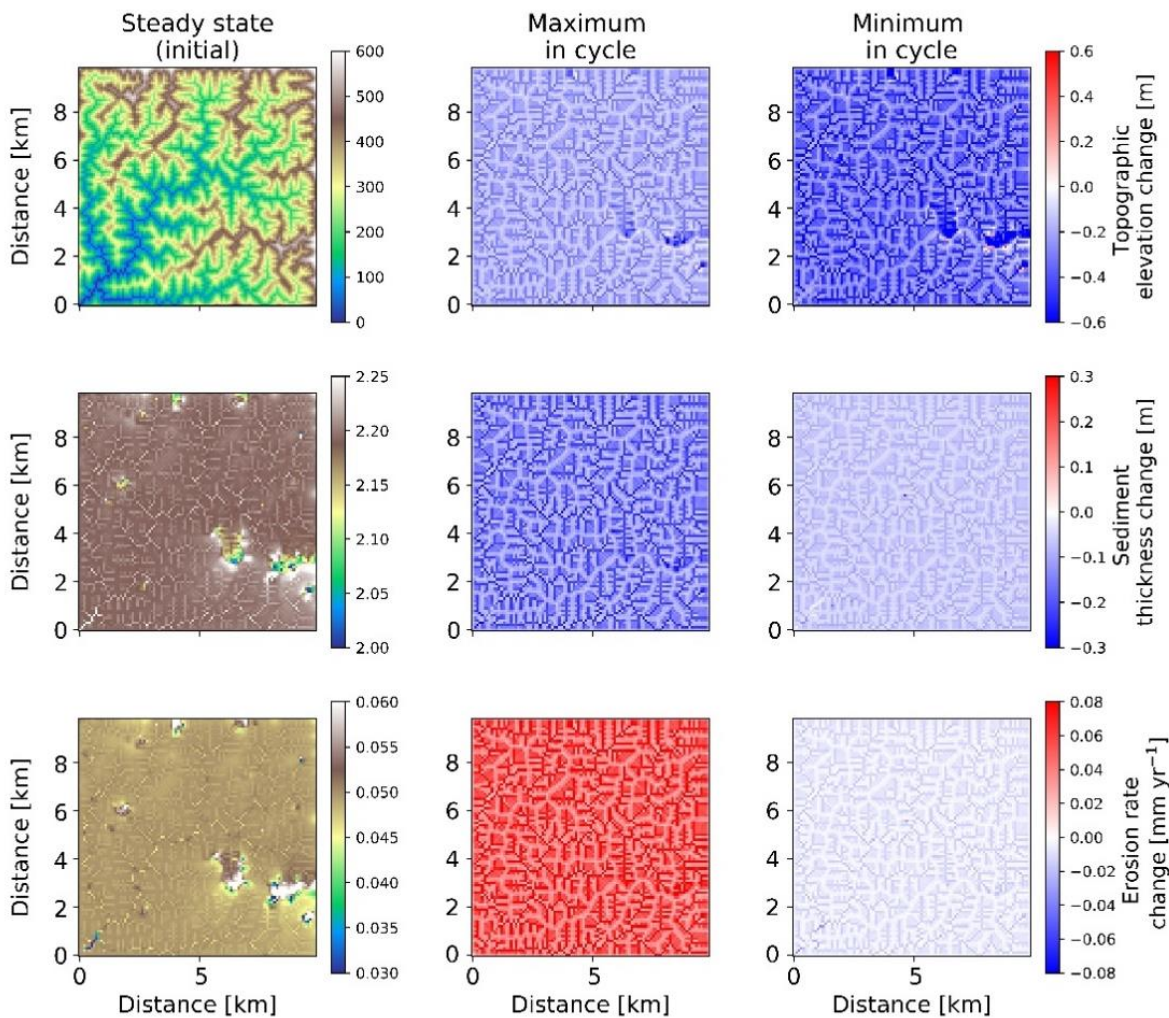
Figure 13. Two-dimensional map-view representation of changes in topographic elevations [m] (1st row), sediment thickness [m] (2nd row), and erosion rates [mm yr⁻¹] (3rd row). These changes are represented with respect to steady state conditions (1st column), for maximum (2nd column) and minimum (3rd column) values of precipitation and vegetation in an oscillation cycle. The simulations represent 70% initial vegetation cover.

In the simulations with dense vegetation cover (70%) (Fig. 13), erosion rate changes from steady state conditions are higher during the maximum ~~u~~in the precipitation and vegetation cover cycle with higher magnitudes (~0.08 mm yr⁻¹ in valleys and up to ~0.02 mm yr⁻¹ on hillslopes and ridges) due to the higher precipitation rates. At minimum precipitation and vegetation cover magnitudes (P = 26 cm; V = 60%), erosion rate changes are reduced (up to -0.03 mm yr⁻¹) in valleys and (up to -0.01 mm yr⁻¹) on hillslopes in comparison to the erosion rates at steady state. Sediment thickness is observed to be relatively higher in the streambeds and valleys (~2.25 m) than the hillslopes. It is contrastingly higher in the lowlands than the areas at higher elevations. At maximum precipitation and vegetation cover (maximum in the cycle) sediment thickness is ~10 cm lower on hillslopes and up to ~30 cm lower in valleys. The same trend with lower amplitude is evident for the minimum in the precipitation and vegetation cover cycle. This implies that at higher vegetation cover, sediment thickness is significantly reduced as a result of higher sediment flux during the peak in precipitation rates. This in turn signifies the dominance of precipitation changes over vegetation cover change in highly vegetated landscapes.

4.6 Comparison to previous studies

Results presented in this study document a higher sensitivity of catchment erosion and sedimentation of sparsely vegetation landscapes (10%) to changes in vegetation cover, whereas densely vegetated (70%) landscapes are more responsive to changes in precipitation than vegetation changes. This confirms the broad findings of Schmid et al. (2018) and Yetemen et al. (2019),

542 which suggest vulnerability of erosion rates in sparsely vegetated landscapes to changes in vegetation cover and, that for

543 densely vegetated landscapes, sensitivity to the changes in MAP. However, there are differences between the results of Schmid

544 et al. (2018) and this study, particularly for the temporal changes in erosion rates we observe for the sparse vegetation cover

545 (10%) scenario with coupled precipitation/vegetation cover oscillations. More specifically, previous results from the

546 detachment limited model shown in Fig. 17 of Schmid et al. (2018) show that catchment erosion rates in sparsely vegetated

547 landscapes decrease as the precipitation and vegetation cover increases in the first part of a cycle. In the second part of the

548 cycle when precipitation and vegetation decrease to their minimum Schmid et al. (2018) predict erosion rates are ~0 mm yr^{-1}.

549 However, in the coupled detachment-transport fluvial erosion model presented here (SPACE), we observe a different behavior

550 and erosion rates slightly increase as precipitation and vegetation cover increase (from 0.05 mm yr^{-1} to 0.065 mm yr^{-1}, Fig.

551 7(e)), rather than decrease. This difference is due to higher sediment entrainment rates we predict during the period of no

552 vegetation and low precipitation (10 mm yr^{-1}), which is a result of higher vulnerability of bare soil to erosion, even with very

553 low precipitation rates. Therefore, the application of a detachment limited, vs. coupled detachment-transport limited modelling

554 approach has bearing on the predicted response, and when comparing results to natural systems care should be taken in which

555 approach is used.

556 Previous geochemistry related observational studies from the Chilean Coastal Cordillera (EarthShape study areas,

557 www.earthshape.net) are also available for comparison to this study. For example, the steady-state sediment thickness in our

558 simulations for 10% and 70% initial vegetation cover are predicted to be higher than the field observations reported by Schaller

559 et al. (2018) and Oeser et al. (2018), who reported a ~20 cm and ~60 cm depth of mobile sediment layers on hillslopes in the

560 Pan de Azucar and La Campana study areas, respectively. Also, the natural topography is steeper, with higher relief and rock

561 uplift rates might be different. Spatial variations in vegetation also occur (e.g., in La Campana), with higher vegetation density

562 along valleys, which might lead to the discrepancies between the observed and predicted sediment thickness. However, the

563 trend in our results (higher sediment thickness for densely vegetated (70%) landscapes) follows the findings of Oeser et al.

564 (2018) who document that sediment increase with increasing mean annual precipitation and vegetation in Chilean Coastal

565 Cordillera. The explanation for the discrepancies between the observed and predicted sediment thickness is unclear to us, but

566 may highlight the need for future improvements in soil production functions used in landscape evolution models.

567 In addition, previous field studies (Oeser et al., 2018; Owen et al., 2011; Schaller et al., 2018) applied cosmogenic nuclides to

568 estimate the denudation and soil production rates in the Chilean Coastal Cordillera. They suggest an increase in soil production

569 rates from arid zones in the north to wet tropical zones in the south of the Chilean Coastal Cordillera. These findings are

570 consistent with the predicted increase in sediment depths (e.g. 1.24 m for V = 10% and 2.22 m for V = 70%, Fig. 7(b)) in our

571 study. Finally, the effects of rock uplift and precipitation rates on topography and erosion rates, as documented by Bonnet and

572 Crave (2003) and Lague et al. (2003) show a linear relationship between mean topographic elevation and rock uplift rate for

573 steady-state conditions.

4.7 Model limitations

575 The model setup used in this study was intended to quantify the sensitivity of hillslope and fluvial erosion, and sediment

576 transport and depositional processes for different climates with variations in precipitation rates and vegetation cover over

577 Milankovitch time scales. This study was designed as an incremental step forward from previous modelling studies (Collins

578 et al., 2004; Guzman, 2019; Istanbulluoglu and Bras, 2005; Istanbulluoglu and Bras, 2006; Schmid et al., 2018).

579 There are several simplifying assumptions made in our modelling approach that warrant discussion and potential investigation

580 in future studies. For example, this study assumed uniform vegetation cover and lithology for the entire catchment. The

581 assumption of uniform vegetation cover in the catchment is likely reasonable given that relatively small (10x10 km^2) size of

catchments investigated and the modest topographic relief produced (between ~75-600m, Fig. 10a). Although temperature and precipitation (and therefore vegetation cover) can vary with elevation, the generally low relief of the catchments in this study do not make this a major concern. Due to the long (geologic) timescales considered in this study and computational considerations, mean annual precipitation rates were applied and stochastic distributions of precipitation could not be considered. While our approach is common for landscape evolution modelling studies conducted on geologic timescales, we recognize that in some settings (such as the arid region of this study, Fig. 1) precipitation events are rare, stochastic in nature, and might have an influence in the results presented here. This is a caveat that warrants future investigation.

The vegetation-erosion parameterization considered in this study follows from that of Istanbulluoglu and Bras (2006) and Schmid et al. (2018). In this parameterization ~~only,~~ the total vegetation cover of the catchment is considered only, rather than the distribution of vegetation cover by individual plant functional types (e.g. grass, shrubs, trees) that would have different Manning's coefficients associated with them. The 'total vegetation cover' approach used in our (and previous) work is a reasonable starting point for understanding landscape evolution over large spatial and temporal scales because: a) more detailed observations about the changes in the distribution of plant functional types over Milankovitch timescales is not available and would be poorly constrained, and b) empirical relationships between total vegetation cover and precipitation are available and easily implemented (e.g. Fig. 2b). However, future work should focus on exploring how the temporal and spatial distribution of different plant functional types during changing climate impacts catchment erosion given that recent work (Mishra et al., 2019; Starke et al., 2020) has identified this as important. This limitation can be handled in future studies with the full coupling of a dynamic vegetation models, such as LPJ-GUESS (Smith et al., 2014; Werner et al., 2018) to a landscape evolution model for the explicit treatment of how different vegetation types change temporally and spatially within a catchment and influence catchment erosion. Also, the 'total vegetation cover' in the model is not disturbed by flow and entrainment, which were observed to have a large impact on the results of Collins et al. (2004) and Istanbulluoglu and Bras (2005). If the vegetation cover was spatio-temporally influenced by above processes in our simulations, the resulting erosion and sedimentation would have been hybrid between sparse (10% V) and densely vegetated (70% V) catchments, with vegetation losses in channels. The time-scale for the current study was based on Milankovitch cycles, to address the effects of periodicity on erosion and sedimentation. However, the effects of seasonal (sub annual) variations in precipitation (Istanbulluoglu and Bras, 2006; Yetemen et al., 2015) and satellite derived vegetation cover (with catchment variable plant function type distributions) also warrant future investigation to identify if coupled seasonal variations in vegetation cover and precipitation influence catchment erosion.

Finally, the results of this study rely upon the vegetation-erosion parameterizations described in section 2 and the appendix (see also Fig. 3). While there is an observational basis for these relationships (see section 1.1, 1.2 in Appendix). There are, frankly, a sparse number of field studies available robustly constraining how different vegetation types and amounts influence hillslope and surface water erosional processes. Thus, we consider the erosional parameterizations used here as hypotheses (rather than robust geomorphic transport laws) that warrant investigation in future field or flume studies.

5 Summary and Conclusions

In this study, we investigate the effects of variable vegetation cover and climate over Milankovitch timescales on catchment scale erosion and sedimentation. Simulations were presented to document if these transients are muted (lower amplitude) at higher rock uplift rates. The approach used here complements previous studies by using a coupled fluvial detachment-transport limited and hillslope diffusion landscape evolution model, and also investigates the degree to which transient effects of vegetation cover and precipitation are measurable in observational studies. The main conclusions deduced from this study are:

i. The step-wise increase in complexity of the model simulations was essential for identifying temporal changes in catchment erosion and sediment thickness. A non-linear response in erosion and sediment thickness to varying precipitation and vegetation cover was observed and results were dependent on the initial vegetation and precipitation state of the catchment. The sources of non-linearity stem from: a) a non-linear relationship between precipitation changes required to cause +/-10% change in vegetation cover (Fig. 2); and b) exponential and power-law relationships in the prescribed vegetation dependent hillslope and fluvial, respectively, geomorphic transport laws (Fig. 3, see also Appendix).

ii. Analysis of results for covarying precipitation and vegetation cover indicate that erosion and sedimentation in densely vegetated landscapes (V = 70%) are more heavily influenced by changes in precipitation than changes in vegetation cover. This is due to the higher amplitude of precipitation change needed to cause variations in vegetation cover in densely vegetated settings (Fig. 5a, 7e).

iii. Analysis of results for covarying precipitation and vegetation cover indicate that erosion and sedimentation in sparsely vegetated landscapes (V = 10%) are more sensitive to variable vegetation cover with constant precipitation rates (Fig. 6, 7e), particular when precipitation rates decrease and vegetation cover approaches 0%.

iv. Concerning the first hypotheses stated in the introduction: We found the effect of Milankovitch periodicity variations on the amplitude of change in sediment thickness and bedrock erosion is more pronounced for longer climate and vegetation oscillations (100 kyr) in both climate and vegetation settings. This finding confirms the hypothesis. Furthermore, periodicity effects on erosion and sediment thickness are larger in densely (70%) vegetated landscapes than sparsely (10%) vegetated landscapes, thereby indicating a sensitivity of the response to the biogeographic zone the changes are imposed on.

v. With respect to our second hypothesis,: all transient forcings in precipitation and vegetation cover explored in this study resulted in variations in erosion and sediment thickness around the mean erosion rate, which is determined by the rock uplift rate. As rock uplift rates increased from 0.05 mm a^{-1} to 0.2 mm a^{-1}, the effects of periodic changes in precipitation and vegetation cover on erosion rates became more pronounced, and were between about 35% to 110%, respectively, of the background rock uplift rate. This finding negates the hypothesis, and suggests that regardless of the tectonic setting considered (within the range of rock uplift rates explored here) erosional transients from varying precipitation and vegetation cover occur, but the detection of these changes requires measurement of erosion rates integrating over short time scales such that the average (tectonically driven) mean erosion rate is not recovered.

vi. Finally, in comparison to previous studies, the 35% to 110% transient changes in erosion rate documented here are at, or above, the detection limit for measurement cosmogenic radionuclides in river sediments preserved in fluvial terraces, but would be undetectable with bedrock thermochronometer dating techniques that average erosion rates over longer timescales. The potential to measure vegetation related transient changes in erosion rates with cosmogenic nuclides is highest in settings with higher rock uplift rates (e.g. 0.1 mm a^{-1}, 0.2 mm a^{-1}) and at longer (41 to 100 kyr) periodicities.

Appendix

1   Effect of vegetation and precipitation on hillslope and fluvial erosion

The approach followed in our study follows the law of continuity of mass (e.g., Tucker et al., 2001). It states that the rate of change in topographic elevation *(z)* is defined as follows:

659 $$\frac{\partial z}{\partial t} = U - \frac{\partial z}{\partial t}(fluvial) + \frac{\partial z}{\partial t}(hillslope),$$ (1)

660 where, U is uplift rate [m yr^{-1}], t is time [yr]. The second and third terms on right-hand side refer to the rate change in
661 topographic elevation due to fluvial and hillslope processes respectively.

1.1 Vegetation dependent hillslope processes

663 The rate of change in topography due to hillslope diffusion (Fernandes and Dietrich, 1997; Martin, 2000) is defined as follows:

664 $$\frac{\partial z}{\partial t}(hillslope) = \nabla q_s,$$ (2)

665 where q_s is sediment flux along the slope S. We applied slope and depth-dependent linear diffusion rule following the approach
666 of Johnstone and Hilley (2014) such that:

667 $$q_s = K_d S d_* \left(1 - e^{-\frac{H}{d_*}}\right),$$ (3)

668 where K_d is diffusion coefficient [m^2 yr^{-1}], d_* is sediment transport decay depth [m], and H denotes sediment thickness.
669 The diffusion coefficient is defined as a function of vegetation cover present on hillslopes, which is estimated following the
670 approach of Istanbulluoglu (2005), Dunne et al. (2010) and (Schmid et al., 2018) as follows:

671 $$K_d = K_b e^{-(\alpha V)},$$ (4)

672 where K_d is defined as a function of vegetation cover V, an exponential decay coefficient α, and linear diffusivity K_b for bare
673 soil.

1.2 Vegetation dependent fluvial processes

675 The fluvial erosion is estimated for a two-layer topography (i.e., bedrock and sediment are treated explicitly) in the coupled
676 detachment – transport limited model, SPACE 1.0 (Shobe et al., 2017). Bedrock erosion and sediment entrainment are
677 calculated simultaneously in the model. Total fluvial erosion is defined as:

678 $$\frac{\partial z}{\partial t}(fluvial) = \frac{\partial R}{\partial t} + \frac{\partial H}{\partial t},$$ (5)

679 where, left-hand side denotes the total fluvial erosion rate. The first and second terms on right-hand side denote the bedrock
680 erosion rate and sediment entrainment rate, respectively.
681 The rate of change of height of bedrock R per unit time [m yr^{-1}] is defined as:

682 $$\frac{\partial R}{\partial t} = U - E_r,$$ (6)

683 where E_r [m yr^{-1}], is the volumetric erosion flux of bedrock per unit bed area.
684 The change in sediment thickness H [m] per unit time [yr] was calculated following Davy and Lague (2009) and Shobe et al.
685 (2017). It is defined as a fraction net deposition rate and solid fraction sediments, as follows:

686 $$\frac{\partial H}{\partial t} = \frac{D_s - E_s}{1 - \emptyset},$$ (7)

687   where, D_s [m yr^{-1}] is the deposition flux of sediment, E_s [m yr^{-1}] is volumetric sediment entrainment flux per unit bed area, and

688   φ is the sediment porosity.

689   Following the approach of Shobe et al. (2017), E_s and E_r given by:

690    $$E_s = (K_s q^m S^n - \omega_{cs})\left(1 - e^{-\frac{H}{H_*}}\right), \tag{8}$$

691    $$E_r = (K_r q^m S^n - \omega_{cr})\, e^{-H/H_*}, \tag{9}$$

692   where, K_s [m^{-1}] and K_r [m^{-1}] are the sediment erodibility and bedrock erodibility parameters respectively. The threshold stream

693   power for sediment entrainment and bedrock erosion are denoted as ω_{cs} [m yr^{-1}] and ω_{cr} [m yr^{-1}] in above equations. Bedrock

694   roughness is denoted as H_* [m] and the term e^{-H/H_*} corresponds to the soil production from bedrock. With higher bedrock

695   roughness magnitudes, more sediment would be produced.

696   K_s and K_r were modified in the model using the approach of Istanbulluoglu (2005) and Schmid et al. (2018) by introducing

697   the effect of Manning's roughness to quantify the effect of vegetation cover on bed shear stress:

698    $$\tau_v = \rho_w g (n_s + n_v)^{6/10} q^m S^n F_t, \tag{10}$$

699   where, ρ_w [kg m^{-3}] and g [m s^{-2}] are the density of water and acceleration due to gravity respectively. Manning's numbers for

700   bare soil and vegetated surface are denoted as n_s and n_v. F_t represents shear stress partitioning ratio. Manning's number for

701   vegetation cover and F_t are calculated as follows:

702    $$n_v = n_{vr}\left(\frac{V}{V_r}\right)^w, \tag{11}$$

703    $$F_t = \left(\frac{n_s}{n_s + n_v}\right)^{\frac{3}{2}}, \tag{12}$$

704   where, n_{vr} is Manning's number for the reference vegetation. Here, V_r is reference vegetation cover *(V = 100%)* and V is local

705   vegetation cover in a model cell, w is empirical scaling factor.

706   Through combining stream power equation (~~Gregory.~~ Tucker et al., 1999; Howard, 1994; Whipple and Tucker, 1999) and the

707   above concept of the effect of vegetation on shear stress, we follow the approach of Schmid et al. (2018) to define new sediment

708   and bedrock erodibility parameters influenced by the surface vegetation cover on fluvial erosion, as follows:

709    $$K_{vs} = K_s \rho_w g (n_s + n_v)^{6/10} F_t, \tag{13}$$

710    $$K_{vr} = K_r \rho_w g (n_s + n_v)^{6/10} F_t, \tag{14}$$

711   where, K_{vs} [m^{-1}] and K_{vr} [m^{-1}] are modified sediment erodibility and bedrock erodibility respectively. These are influenced by

712   fractional vegetation cover V. Hence, K_s and K_r in Eq. (8) and Eq. (9) are replaced by K_{vs} and K_{vr} to include an effect of

713   vegetation cover on fluvial processes in the model. The trends of K_d, K_{vs} and K_{vr} are illustrated in Fig. 3.

714   **2. Influence of coupled oscillations of precipitation and vegetation cover, on erosion and sedimentation (Scenario 3)**

715   **without weathering function**

716
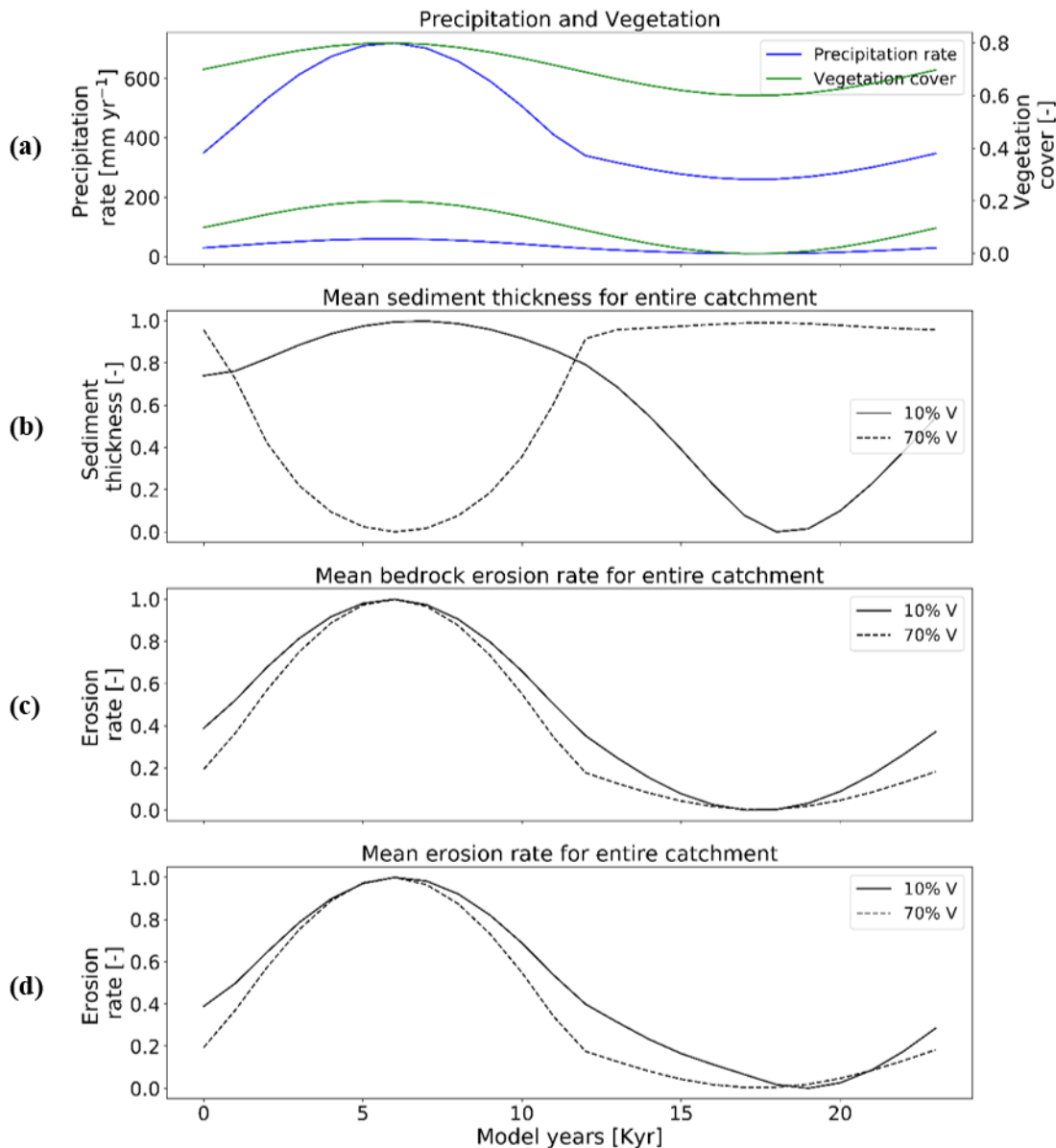
Figure A1: Temporal evolution of catchment averaged predictions for scenario 3 (with no weathering) described in the text (section
3.3). Graphical representation of normalized mean catchment sedimentation and erosion to (a) coupled oscillations in precipitation
[mm yr⁻¹] and vegetation cover [-] in terms of (b) sediment thickness [-], (c) bedrock erosion [-], (d) mean erosion rate [-] for entire
catchment. The periodicity of climate and vegetation oscillations is 23 kyr with rate of rock uplift as 0.5 mm yr⁻¹.

Code availability

The code and data used in this study are freely available upon request.

Author contributions

HS and TAE designed the initial model setup and simulation programs. HS and TAE conducted model modifications,
simulation runs and analysis. MS provided assistance in program modification. KT provided insight into plant ecology in
Chilean Study areas and vegetation-climate change relationships. HS and TAE prepared the manuscript with contributions
from C.G., KT, and MS.

Competing interests

The authors declare that they have no competing interests.

Acknowledgements

H.S and T.A.E. acknowledge support by Open Access Publishing Fund of University of Tübingen. We also acknowledge support from the Research Training Group 1829 Integrated Hydrosystem Modelling, funded by the German Research Foundation (DFG). In addition, T.A.E, K.T. and M.S. acknowledge support from the German priority research program (SPP-1803; grants EH329/14-1 and EH329/14-2 to T.A.E, and TI 338/14-1 and TI338/14-2 to K.T.). We thank Erkan Istanbulluoglu and Omer Yetemen for their constructive reviews.

References

Acosta, V. T., Schildgen, T. F., Clarke, B. A., Scherler, D., Bookhagen, B., Wittmann, H., von Blanckenburg, F., and Strecker, M. R.: Effect of vegetation cover on millennial-scale landscape denudation rates in East Africa, 7, 408–420, https://doi.org/10.1130/l402.1, 2015.

Ahnert, F.: Some comments on the quantitative formulation of geomorphological processes in a theoretical model, 2, 191–201, https://doi.org/10.1002/esp.3290020211, 1977.

Alonso, R. N., Bookhagen, B., Carrapa, B., Coutand, I., Haschke, M., Hilley, G. E., Schoenbohm, L., Sobel, E. R., Strecker, M. R., Trauth, M. H., and Villanueva, A.: Tectonics, Climate, and Landscape Evolution of the Southern Central Andes: the Argentine Puna Plateau and Adjacent Regions between 22 and 30°S, in: The Andes: Active Subduction Orogeny, edited by: Oncken, O., Chong, G., Franz, G., Giese, P., Götze, H.-J., Ramos, V. A., Strecker, M. R., and Wigger, P., Springer Berlin Heidelberg, Berlin, Heidelberg, 265–283, 2006.

Amundson, R., Heimsath, A., Owen, J., Yoo, K., and Dietrich, W. E.: Hillslope soils and vegetation, 234, 122–132, https://doi.org/10.1016/j.geomorph.2014.12.031, 2015.

Ashkenazy, Y., Eisenman, I., Gildor, H., and Tziperman, E.: The Effect of Milankovitch Variations in Insolation on Equatorial Seasonality, Journal of Climate, 23, 6133–6142, https://doi.org/10.1175/2010JCLI3700.1, 2010.

Avdievitch, N. N., Ehlers, T. A., and Glotzbach, C.: Slow Long-Term Exhumation of the West Central Andean Plate Boundary, Chile, 37, 2243–2267, https://doi.org/10.1029/2017TC004944, 2018.

Bellard, C., Bertelsmeier, C., Leadley, P., Thuiller, W., and Courchamp, F.: Impacts of climate change on the future of biodiversity, Ecology Letters, 15, 365–377, https://doi.org/10.1111/j.1461-0248.2011.01736.x, 2012.

Bonnet, S. and Crave, A.: Landscape response to climate change: Insights from experimental modeling and implications for tectonic versus climatic uplift of topography, 31, 123–126, https://doi.org/10.1130/0091-7613(2003)031<0123:Lrtcci>2.0.Co;2, 2003.

Braun, J., Voisin, C., Gourlan, A. T., and Chauvel, C.: Erosional response of an actively uplifting mountain belt to cyclic rainfall variations, Earth Surf. Dynam., 3, 1–14, https://doi.org/10.5194/esurf-3-1-2015, 2015.

760 Breckle, S.-W.: Walter's Vegetation of the Earth, 4th ed., Springer-Verlag Berlin Heidelberg, XX, 527 pp., 2002.

761 Collins, D. B. G., Bras R. L., and Tucker G. E.: Modeling the effects of vegetation-erosion coupling on landscape evolution,
762 109, https://doi.org/10.1029/2003jf000028, 2004.

763 Dixon, J. L., Heimsath, A. M., and Amundson, R.: The critical role of climate and saprolite weathering in landscape evolution,
764 34, 1507–1521, https://doi.org/10.1002/esp.1836, 2009.

765 van Dongen, R., Scherler, D., Wittmann, H., and von Blanckenburg, F.: Cosmogenic ^{10}Be in river
766 sediment: where grain size matters and why, 1–31, https://doi.org/10.5194/esurf-2018-83, 2018.

767 Dosseto, A., Hesse, P. P., Maher, K., Fryirs, K., and Turner, S.: Climatic and vegetation control on sediment dynamics during
768 the last glacial cycle, 38, 395–398, https://doi.org/10.1130/g30708.1, 2010.

769 Gerten, D., Luo, Y., Le Maire, G., Parton, W. J., KEOUGH, C., WENG, E., BEIER, C., CIAIS, P., CRAMER, W., DUKES,
770 J. S., HANSON, P. J., KNAPP, A. A. K., LINDER, S., NEPSTAD, D., RUSTAD, L., and SOWERBY, A.: Modelled effects
771 of precipitation on ecosystem carbon and water dynamics in different climatic zones, Global Change Biology, 14, 2365–2379,
772 https://doi.org/10.1111/j.1365-2486.2008.01651.x, 2008.

773 Gilbert, G. K.: Report on the geology of the Henry Mountains, Washington, D.C., https://doi.org/10.3133/70039916, 1877.

774 ~~Guzman, C. D.: Hillslope sediment transport across climates and vegetative influences, 47, 495–496,~~
775 ~~https://doi.org/10.1130/focus052019.1, 2019.~~

776 Hancock, G. S. and Anderson, R. S.: Numerical modeling of fluvial strath-terrace formation in response to oscillating climate,
777 114, 1131–1142, https://doi.org/10.1130/0016-7606(2002)114<1131:NMOFST>2.0.CO;2, 2002.

778 Heimsath, A. M., Dietrich, W. E., Nishiizumi, K., and Finkel, R. C.: The soil production function and landscape equilibrium,
779 Nature, 388, 358–361, https://doi.org/10.1038/41056, 1997.

780 Herman, F., Rhodes, E. J., Braun, J., and Heiniger, L.: Uniform erosion rates and relief amplitude during glacial cycles in the
781 Southern Alps of New Zealand, as revealed from OSL-thermochronology, Earth and Planetary Science Letters, 297, 183–189,
782 https://doi.org/10.1016/j.epsl.2010.06.019, 2010.

783 Hobley, D. E. J., Adams, J. M., Nudurupati, S. S., Hutton, E. W. H., Gasparini, N. M., Istanbulluoglu, E., and Tucker, G. E.:
784 Creative computing with Landlab: an open-source toolkit for building, coupling, and exploring two-dimensional numerical
785 models of Earth-surface dynamics, 5, 21–46, https://doi.org/10.5194/esurf-5-21-2017, 2017.

786 Howard, A. D.: A detachment-limited model of drainage basin evolution, 2261–2285, 1994.

787 Huntley, B., Allen, J. R., Collingham, Y. C., Hickler, T., Lister, A. M., Singarayer, J., Stuart, A. J., Sykes, M. T., and Valdes,
788 P. J.: Millennial climatic fluctuations are key to the structure of last glacial ecosystems, 8, e61963,
789 https://doi.org/10.1371/journal.pone.0061963, 2013.

790 Huxman, T. E., Smith, M. D., Fay, P. A., Knapp, A. K., Shaw, M. R., Loik, M. E., Smith, S. D., Tissue, D. T., Zak, J. C.,
791 Weltzin, J. F., Pockman, W. T., Sala, O. E., Haddad, B. M., Harte, J., Koch, G. W., Schwinning, S., Small, E. E., and Williams,

D. G.: Convergence across biomes to a common rain-use efficiency, Nature, 429, 651–654, https://doi.org/10.1038/nature02561, 2004.

Hyun, S., Ahagon, N., and Yoon, H.-I.: Milankovitch cycles and paleoceanographic evolution within sediments from ODP Sites 980 and 983 of the North Atlantic Ocean, 9, 235, https://doi.org/10.1007/BF02910583, 2005.

Istanbulluoglu, E. and Bras, R. L.: Vegetation-modulated landscape evolution: Effects of vegetation on landscape processes, drainage density, and topography, 110, https://doi.org/10.1029/2004jf000249, 2005.

Istanbulluoglu, E. and Bras, R. L.: On the dynamics of soil moisture, vegetation, and erosion: Implications of climate variability and change, 42, https://doi.org/10.1029/2005wr004113, 2006.

Jeffery, M. L., Yanites, B. J., Poulsen, C. J., and Ehlers, T. A.: Vegetation-precipitation controls on Central Andean topography, 119, 1354–1375, https://doi.org/10.1002/2013jf002919, 2014.

Johnstone, S. A. and Hilley, G. E.: Lithologic control on the form of soil-mantled hillslopes, 43, 83–86, https://doi.org/10.1130/g36052.1, 2014.

Kelly, A. E. and Goulden, M. L.: Rapid shifts in plant distribution with recent climate change, Proc Natl Acad Sci USA, 105, 11823, https://doi.org/10.1073/pnas.0802891105, 2008.

Kirby, E. and Whipple, K. X.: Expression of active tectonics in erosional landscapes, 44, 54–75, https://doi.org/10.1016/j.jsg.2012.07.009, 2012.

Knapp, A. K., Ciais, P., and Smith, M. D.: Reconciling inconsistencies in precipitation–productivity relationships: implications for climate change, New Phytologist, 214, 41–47, https://doi.org/10.1111/nph.14381, 2017.

Kojima, S., Soto, I., Quiroz, M., Valencia, P., and Fernandez, I.: Geological and Geochemical Characteristics of the Intrusion-Related Vein-Type Gold Deposits in the El Morado District, Coastal Cordillera, Northern Chile, 67, 197–206, https://doi.org/10.1111/rge.12129, 2017.

Lague, D., Crave, A., and Davy, P.: Laboratory experiments simulating the geomorphic response to tectonic uplift, 108, ETG 3-1-ETG 3-20, https://doi.org/10.1029/2002jb001785, 2003.

McPhillips, D., Bierman, P. R., Crocker, T., and Rood, D. H.: Landscape response to Pleistocene-Holocene precipitation change in the Western Cordillera, Peru:10Be concentrations in modern sediments and terrace fills, 118, 2488–2499, https://doi.org/10.1002/2013jf002837, 2013.

Melnick, D.: Rise of the central Andean coast by earthquakes straddling the Moho, 9, 401–407, https://doi.org/10.1038/ngeo2683, 2016.

Miller, S. R., Sak, P. B., Kirby, E., and Bierman, P. R.: Neogene rejuvenation of central Appalachian topography: Evidence for differential rock uplift from stream profiles and erosion rates, 369–370, 1–12, https://doi.org/10.1016/j.epsl.2013.04.007, 2013.

Mishra, A. K., Placzek, C., and Jones, R.: Coupled influence of precipitation and vegetation on millennial-scale erosion rates derived from 10Be, 14, e0211325, https://doi.org/10.1371/journal.pone.0211325, 2019.

Mowll, W., Blumenthal, D. M., Cherwin, K., Smith, A., Symstad, A. J., Vermeire, L. T., Collins, S. L., Smith, M. D., and Knapp, A. K.: Climatic controls of aboveground net primary production in semi-arid grasslands along a latitudinal gradient portend low sensitivity to warming, Oecologia, 177, 959–969, https://doi.org/10.1007/s00442-015-3232-7, 2015.

Oeser, R. A., Stroncik, N., Moskwa, L.-M., Bernhard, N., Schaller, M., Canessa, R., van den Brink, L., Köster, M., Brucker, E., Stock, S., Fuentes, J. P., Godoy, R., Matus, F. J., Oses Pedraza, R., Osses McIntyre, P., Paulino, L., Seguel, O., Bader, M. Y., Boy, J., Dippold, M. A., Ehlers, T. A., Kühn, P., Kuzyakov, Y., Leinweber, P., Scholten, T., Spielvogel, S., Spohn, M., Übernickel, K., Tielbörger, K., Wagner, D., and von Blanckenburg, F.: Chemistry and microbiology of the Critical Zone along a steep climate and vegetation gradient in the Chilean Coastal Cordillera, CATENA, 170, 183–203, https://doi.org/10.1016/j.catena.2018.06.002, 2018.

Owen, J. J., Amundson, R., Dietrich, W. E., Nishiizumi, K., Sutter, B., and Chong, G.: The sensitivity of hillslope bedrock erosion to precipitation, 36, 117–135, https://doi.org/10.1002/esp.2083, 2011.

Pelletier, J. D.: Fluvial and slope-wash erosion of soil-mantled landscapes: detachment- or transport-limited?, 37, 37–51, https://doi.org/10.1002/esp.2187, 2012.

Perron, J. T.: Climate and the Pace of Erosional Landscape Evolution, 45, 561–591, https://doi.org/10.1146/annurev-earth-060614-105405, 2017.

Rossel, K., Aguilar, G., Salazar, E., Martinod, J., Carretier, S., Pinto, L., and Cabré, A.: Chronology of Chilean Frontal Cordillera building from geochronological, stratigraphic and geomorphological data insights from Miocene intramontane-basin deposits, 30, 289–310, https://doi.org/10.1111/bre.12221, 2018.

Routschek, A., Schmidt, J., and Kreienkamp, F.: Impact of climate change on soil erosion — A high-resolution projection on catchment scale until 2100 in Saxony/Germany, 121, 99–109, https://doi.org/10.1016/j.catena.2014.04.019, 2014.

Sala, O. E., Parton, W. J., Joyce, L. A., and Lauenroth, W. K.: Primary Production of the Central Grassland Region of the United States, Ecology, 69, 40–45, https://doi.org/10.2307/1943158, 1988.

Schaller, M. and Ehlers, T. A.: Limits to quantifying climate driven changes in denudation rates with cosmogenic radionuclides, 248, 153–167, https://doi.org/10.1016/j.epsl.2006.05.027, 2006.

Schaller, M., Blanckenburg, F. von, Hovius, N., Veldkamp, A., van den Berg, M. W., and Kubik, P. W.: Paleoerosion Rates from Cosmogenic 10Be in a 1.3 Ma Terrace Sequence: Response of the River Meuse to Changes in Climate and Rock Uplift, The Journal of Geology, 112, 127–144, https://doi.org/10.1086/381654, 2004.

Schaller, M., Ehlers, T. A., Lang, K. A. H., Schmid, M., and Fuentes-Espoz, J. P.: Addressing the contribution of climate and vegetation cover on hillslope denudation, Chilean Coastal Cordillera (26°–38°S), 489, 111–122, https://doi.org/10.1016/j.epsl.2018.02.026, 2018.

Schaller, M., Dal Bo, I., Ehlers, T. A., Klotzsche, A., Drews, R., Fuentes Espoz, J. P., and van der Kruk, J.: Comparison of regolith physical and chemical characteristics with geophysical data along a climate and ecological gradient, Chilean Coastal Cordillera (26 to 38\degree\,S), 6, 629–647, https://doi.org/10.5194/soil-6-629-2020, 2020.

Schmid, M., Ehlers, T. A., Werner, C., Hickler, T., and Fuentes-Espoz, J.-P.: Effect of changing vegetation and precipitation on denudation – Part 2: Predicted landscape response to transient climate and vegetation cover over millennial to million-year timescales, 6, 859–881, https://doi.org/10.5194/esurf-6-859-2018, 2018.

Seybold, H., Rothman, D. H., and Kirchner, J. W.: Climate's watermark in the geometry of stream networks, 44, 2272–2280, https://doi.org/10.1002/2016gl072089, 2017.

Shobe, C. M., Tucker, G. E., and Barnhart, K. R.: The SPACE 1.0 model: A Landlab component for 2-D calculation of sediment transport, bedrock erosion, and landscape evolution, 1–38, https://doi.org/10.5194/gmd-2017-175, 2017.

Slater, L. J. and Singer, M. B.: Imprint of climate and climate change in alluvial riverbeds: Continental United States, 1950-2011, 41, 595–598, https://doi.org/10.1130/g34070.1, 2013.

Smith, B., W\aarlind, D., Arneth, A., Hickler, T., Leadley, P., Siltberg, J., and Zaehle, S.: Implications of incorporating N cycling and N limitations on primary production in an individual-based dynamic vegetation model, 11, 2027–2054, https://doi.org/10.5194/bg-11-2027-2014, 2014.

Smith, M. D., Wilcox, K. R., Power, S. A., Tissue, D. T., and Knapp, A. K.: Assessing community and ecosystem sensitivity to climate change – toward a more comparative approach, Journal of Vegetation Science, 28, 235–237, https://doi.org/10.1111/jvs.12524, 2017.

Starke, J., Ehlers, T. A., and Schaller, M.: Latitudinal effect of vegetation on erosion rates identified along western South America, Science, 367, 1358, https://doi.org/10.1126/science.aaz0840, 2020.

Tucker, G. E.: Drainage basin sensitivity to tectonic and climatic forcing: implications of a stochastic model for the role of entrainment and erosion thresholds, 29, 185–205, https://doi.org/10.1002/esp.1020, 2004.

Tucker, G. E., Gasparini, N. M., Lancaster, S. T., and Bras, R. L.: Modeling Floodplain Dynamics and Stratigraphy: Implications for Geoarchaeology, 1999.

Turowski, J. M., Lague, D., Crave, A., and Hovius, N.: Experimental channel response to tectonic uplift, 111, n/a-n/a, https://doi.org/10.1029/2005jf000306, 2006.

Werner, C., Schmid, M., Ehlers, T. A., Fuentes-Espoz, J. P., Steinkamp, J., Forrest, M., Liakka, J., Maldonado, A., and Hickler, T.: Effect of changing vegetation and precipitation on denudation – Part 1: Predicted vegetation composition and cover over the last 21 thousand years along the Coastal Cordillera of Chile, 6, 829–858, https://doi.org/10.5194/esurf-6-829-2018, 2018.

Whipple, K. X.: The influence of climate on the tectonic evolution of mountain belts, Nature Geoscience, 2, 730–730, https://doi.org/10.1038/ngeo638, 2009.

Whipple, K. X. and Tucker, G. E.: Dynamics of the stream-power river incision model: Implications for height limits of mountain ranges, landscape response timescales, and research needs, 104, 17661–17674, https://doi.org/10.1029/1999jb900120, 1999.

Willgoose, G., Bras, R. L., and Rodriguez-Iturbe, I.: A coupled channel network growth and hillslope evolution model: 1. Theory, 27, 1671–1684, https://doi.org/10.1029/91WR00935, 1991.

Xia, J., Chen, J., Piao, S., Ciais, P., Luo, Y., and Wan, S.: Terrestrial carbon cycle affected by non-uniform climate warming, Nature Geoscience, 7, 173–180, https://doi.org/10.1038/ngeo2093, 2014.

Yang, Y., Fang, J., ma, W., and Wang, W.: Relationship between variability in aboveground net primary production and precipitation in global grasslands. Geophysical Research Letters, Geophysical Research Letters - GEOPHYS RES LETT, 35, https://doi.org/10.1029/2008GL035408, 2008.

Yanites, B. J. and Ehlers, T. A.: Global climate and tectonic controls on the denudation of glaciated mountains, Earth and Planetary Science Letters, 325–326, 63–75, https://doi.org/10.1016/j.epsl.2012.01.030, 2012.

Yetemen, O., Istanbulluoglu, E., and Duvall, A. R.: Solar radiation as a global driver of hillslope asymmetry: Insights from an ecogeomorphic landscape evolution model, Water Resources Research, 51, 9843–9861, https://doi.org/10.1002/2015WR017103, 2015.

Yetemen, O., Saco, P. M., and Istanbulluoglu, E.: Ecohydrology Controls the Geomorphic Response to Climate Change, Geophysical Research Letters, 46, 8852–8861, https://doi.org/10.1029/2019GL083874, 2019.

Zhang, Y., Xiao, X., Guanter, L., Zhou, S., Ciais, P., Joiner, J., Sitch, S., Wu, X., Nabel, J., Dong, J., Kato, E., Jain, A. K., Wiltshire, A., and Stocker, B. D.: Precipitation and carbon-water coupling jointly control the interannual variability of global land gross primary production, Scientific Reports, 6, 39748, https://doi.org/10.1038/srep39748, 2016.